# PHOTOVOLTAIC POWERED ELECTRIC MOTOR DRIVES

DISSERTATION

SUBMITTED IN PARTIAL FULFILLMENT OF THE REQUIREMENTS

FOR THE AWARD OF THE DEGREE

OF

MASTER OF TECHNOLOGY

IN

CONTROL & INSTRUMENTATION

SUBMITTED BY:

**Saumya Singh**

**(2K12/ C&I/ 016)**

UNDER THE SUPERVISION OF

**Dr. Dheeraj Joshi**

**DEPARTMENT OF ELECTRICAL ENGINEERING**

DELHI TECHNOLOGICAL UNIVERSITY

(Formerly Delhi College of Engineering)

Bawana Road, Delhi-110042

INDIA

2014

# DEPARTMENT OF ELECTRICAL ENGINEERING

DELHI TECHNOLOGICAL UNIVERSITY

(Formerly Delhi College of Engineering)

Bawana Road, Delhi-110042

INDIA

## CERTIFICATE

I, **Saumya Singh**, Roll No. 2K12/C&I/016, a student of M. Tech. (Control & Instrumentation), hereby declare that the dissertation titled "**Photovaoltaic Powered Electric Motor Drives**" is a bonafide record of the work carried out by me under the supervision of **Dr. Dheeraj Joshi** of Electrical Engineering Department, Delhi Technological University in partial fulfilment of the requirement for the award of the degree of Master of Technology and has not been submitted elsewhere for the award of any other Degree or diploma.

**(Saumya Singh)**

**Place: DTU, Delhi**

**Date :**

**Signature of supervisor**

**Dr Dheeraj Joshi**

**Associate Professor [EED]**

# ACKNOWLEDGEMENT

I take this as an opportunity to thank and express my deepest gratitude to everyone who has played a part and contributed in the successful completion of this Dissertation. Apart from my efforts, the success of this project depends mostly on the motivation, help and guidelines provided by my supervisor and friends. Without their support and belief in me, this work would not have been successful.

I would like to show my greatest admiration for my supervisor Dr. Dheeraj Joshi. I thank him for his tremendous support and help. I felt motivated, enlightened and encouraged every time I met him with my doubts and queries. Without his words of wisdom and guidance this dissertation would not have been possible.

The guidance and support received from all friends and colleagues, who contributed and helped in this project, have been vital for the success of this work. I am grateful for their invariable support and unconditional assistance.

Delhi, 2014 SAUMYA SINGH

# ABSTRACT

This dissertation presents speed control of DC and induction motor powered by photovoltaic panel. For a fixed radiation and temperature the amount of power developed by the panel is fixed, and MPPT is employed to attain maximum power out of this. Duty cycle is generated for switching of MOSFET and IGBT in boost circuit. Boost converter circuit is usually employed to attain the voltage equal to the rated motor voltage.

Apart from this vector control of induction motor has been in focus the motor flux and torque is controlled independently as a result motor behaves like separately excited DC motor.

With introduction of controllers the speed of motor is retained at rated speed even if load is applied to both DC and induction motor. The different types of controller used are PI controller, Fuzzy logic controller and ANFIS controller. The simulation results of these controllers are discussed in detail. MATLAB 7.10.0(R2010a) is used for simulation purpose.

# CONTENTS

# LIST OF FIGURES

## LIST OF TABLES

# LIST OF SYMBOLS AND ABBREVIATIONS

| | |
|---|---|
| q | Electron charge |
| k | Boltzmann constant |
| $I_{sc}(T_1)$ | Module short circuit current at $25^0$C |
| G | The irradiation on the surface of device. |
| T | The actual temperature in Kelvin. |
| $N_p$ | Number of cells in parallel connection |
| $N_s$ | Number of cells in series connection |
| $V_{pv}$ | Output voltage of PV module |
| A | Ideality factor |
| $R_s$ | Series resistance of the cell |
| $V_{in\ (min)}$ & $V_{in\ (max)}$ | Input voltage Range |
| $V_{out}$ | Nominal Output Voltage |
| $I_{out\ (max)}$ | Maximum Output Current |
| **η** | efficiency of boost converter |
| D | Duty cycle |
| $\Delta I_L$ | calculated inductor ripple current |
| $I_{out\ (max)}$ | maximum output current necessary in the application |
| L | selected inductor value |
| $f_s$ | minimum switching frequency |
| $I_{SW(max)}$ | maximum switch current in the system |
| $I_f$ | average forward current of diode rectifier |
| $\Delta V_{out}$ | desired output voltage ripple |
| $C_{out}$ | Minimum output capacitance |

| | |
|---|---|
| I | current through armature winding |
| $w_m$ | speed of the motor |
| η, | Efficiency |
| P | density (Kg/m3) |
| G | acceleration of gravity ($m^2$/s) |
| H | head(m) |
| Q | flow(m3/S) |
| $\Delta i$ | hysteresis band limit |
| S | Small |
| M | Medium |
| L | Large |
| VL | Very Large |
| PVVL | Positive Very Very Large |
| VVL | Very Very Large |

# CHAPTER I

# INTRODUCTION

## 1.1 GENERAL

India with the world's second largest population and fourth in terms of purchasing power is a rapidly emerging economy. India is sufficient in amount of primary energy sources such as fossil, renewable and other new energy sources. The share of coal is the highest in power sector industries and also in country's electricity mix with a robust 59% share, followed by hydroelectricity at 17%, Renewable energy at 12%, Natural gas at9% and the remaining part is contributed by nuclear energy and oil which stands at 2% and less than 1% respectively. The distribution of the consumption patterns and production profile do not match in terms of primary sources, creating concerns about energy security. Figure 1.1 shows the source wise estimated electricity potential.

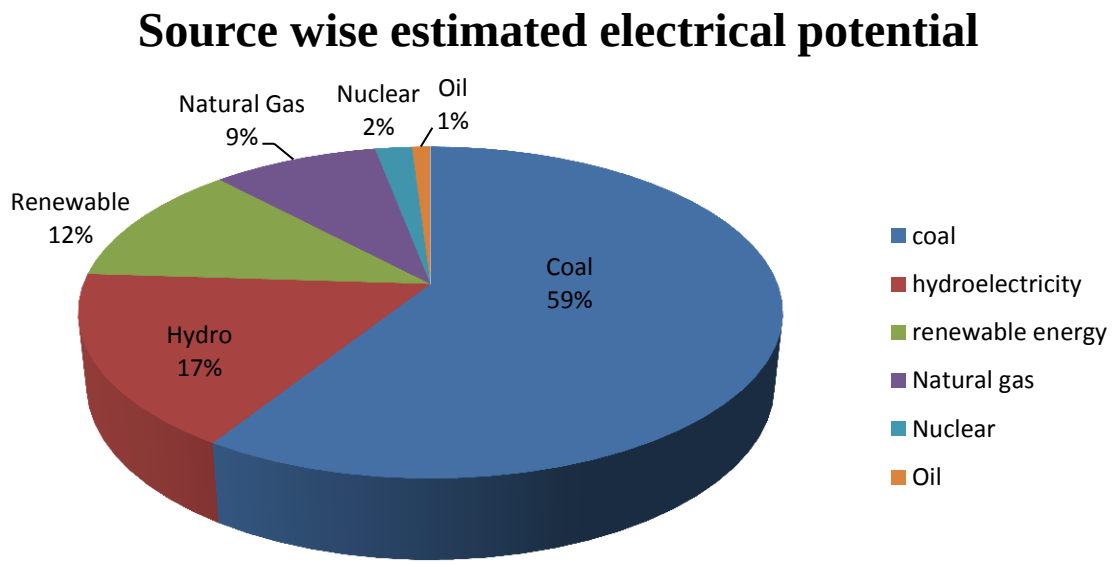


**Fig.1.1 Share of Different Energy Sources**

India's electricity consumption per capita is around 778 KWh and is much less than other countries or places in the world. About 80% of Indian rural areas are said to be getting electricity supply but in real terms around 33% houses in rural areas and 6% of the urban areas do not get frequent electricity supply. This adds up to a total of 300 million houses in the country devoid of any access to electricity in absolute terms. Electricity usage in the country is estimated to grow up to2290 billion kWh by 2022-23 and up to 4510billion kWh by2032-33. Wood and kerosene are the basic fuels used by most of the rural population to fulfill their energy needs as they do not have access to uninterrupted and stable energy source. India is facing the problem of huge demand supply gap leading to darkness. The supply is 778 billion kilowatt-hours (kWh) compared to huge of demand of 890 billion kWh and is expected to increase to 1450 billion kWh by April 2017.

As the energy demand is increasing and the non-availability of conventional sources to meet the power demand day by day is also increasing causing great concern towards power sector. The unabated exploitation of fossil resources has resulted in huge reduction in their deposits and also caused global warming to further. Therefore, the present global scenario has led to increase in demand of renewable energy sources to be developed apart from conventional system of energy to satisfy the power demand. Non-conventional energy sources like solar energy and wind energy are the most effectively being utilized in this context. The photo Voltaire energy source is the major energy resource that is a clean power gaining much significance as the world is shifting towards greener source to meet its energy demand.

Of the total 31,151.03 MW renewable power installed in India, 66.8% is power through wind energy. Next major source of renewable energy is hydro power, which constitutes nearly 12.4% of renewable energy. With huge potential and 7.6% share of total installed renewable energy, solar power stands 3$^{rd}$ most important source of renewable

energy in India. Other notable sources are power through biomass and waste as shown in Fig.1.2.

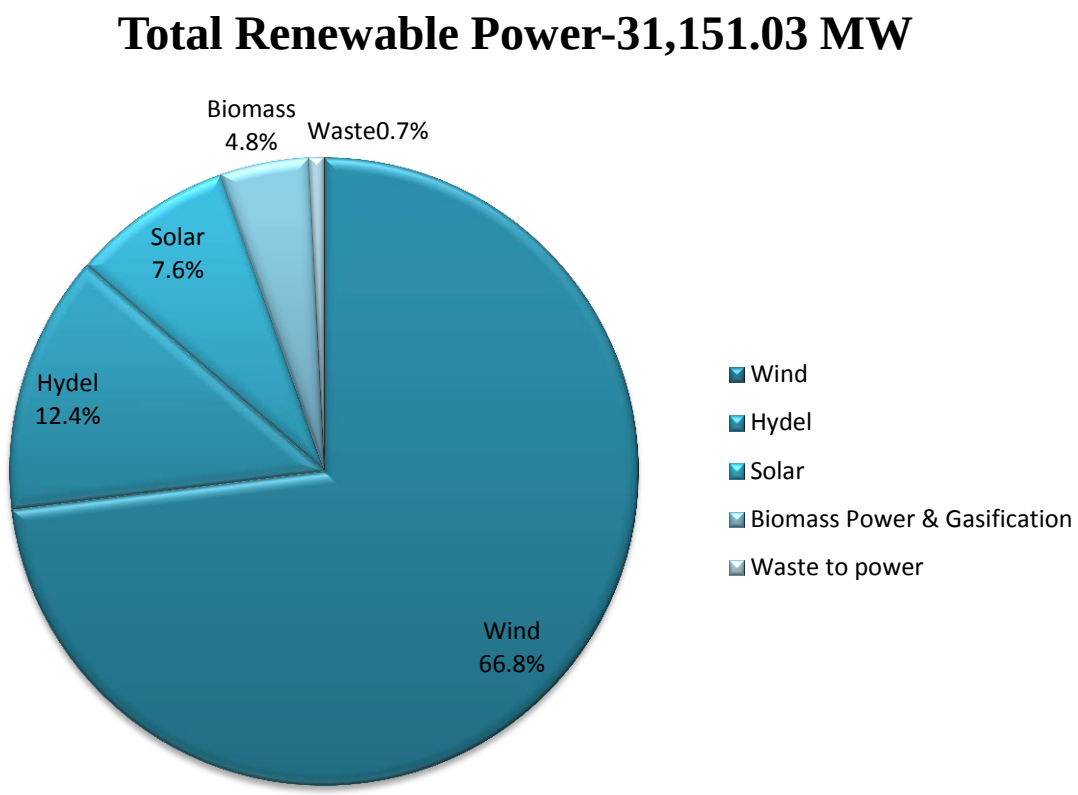


**Fig-1.2 Share Of different Renewable energy sources**

India is blessed with abundance of solar energy if used in an efficient way, India's energy demands can be met to a great extent without much effort. On a sunny day solar illumination is more than 1000w/$m^2$over Indian subcontinent. India is showing great commitment for increasing the % share power or electricity generation through renewable sources every year and expected to reach to 16% by 2022. Indian power sector is having a huge gap in demand and supply which can be easily met if various changes in current setup are made and emphasis is on greener sources of power generation. To reduce this perennial energy shortage the Jawaharlal Nehru National Solar Mission (JNNSM) is launched which is a joint initiative of the Ministry of New and Renewable Energy and Ministry of Power. It is among the many significant environment friendly energy solutions available in India.

This has a target of 20,000 MW on grid connection of solar power generated and 2000 MW generation should be off-grid capacity inclusive of 2 crores solar lit systems and 2 crores meters square collection area of thermal energy from the sun. From last year few years' states of Gujarat and Madhya Pradesh have taken many new steps in the field of solar energy. Grid –connected solar plants in 2011, crossed100MW generation. The wind energy sector is the major Renewable energy source it also showcased huge potential by generating around 3000 MW capacities resulting in increase of wind energy share for each 22,000 MW milestones.

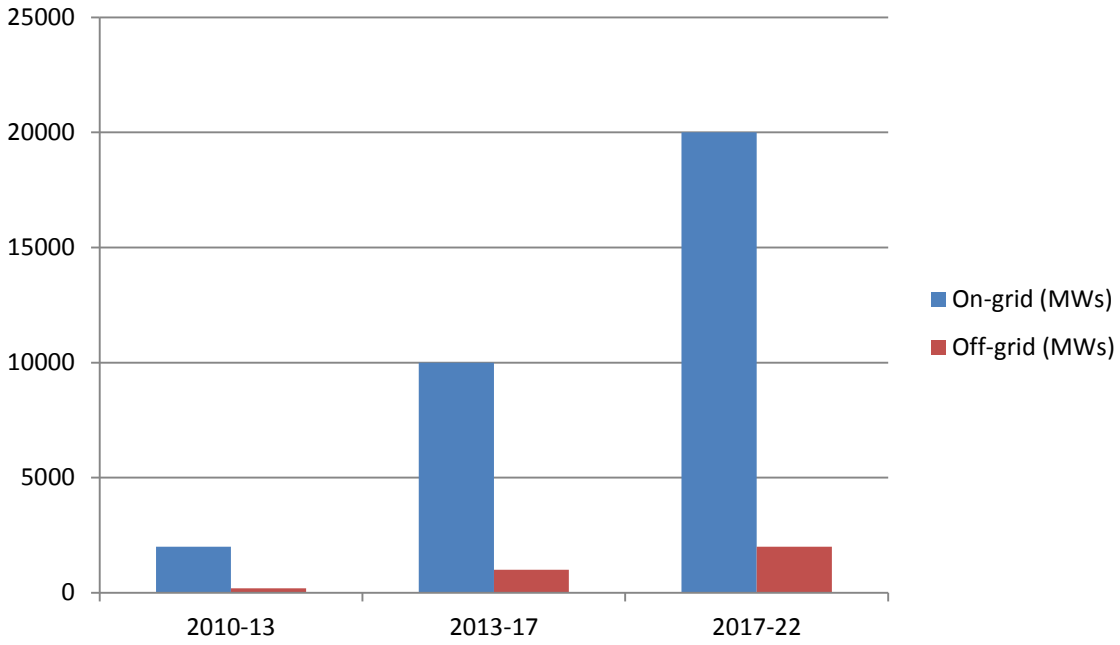


**Fig-1.3 Growth Trend of Jawaharlal National Solar Mission.**

Electrical power generation through solar energy or photovoltaic process is the process of converting light energy into electricity based completely on solid state materials (i.e. semiconductors). This process of energy generation is greener and cleaner source of energy as there is no fuel required and pollutants are not emitted. There are no rotational

losses as there are no moving parts. They can either be separate generation unit or can be grid connected generation unit. This depends on whether the nearby grid is available or not. Another major advantage of using solar power is the portability of plant wherever and whenever operation is required and least affected by environmental factors like snow, winds etc. However they do not produce electricity on cloudy days or during night, then other energy sources can be switched.

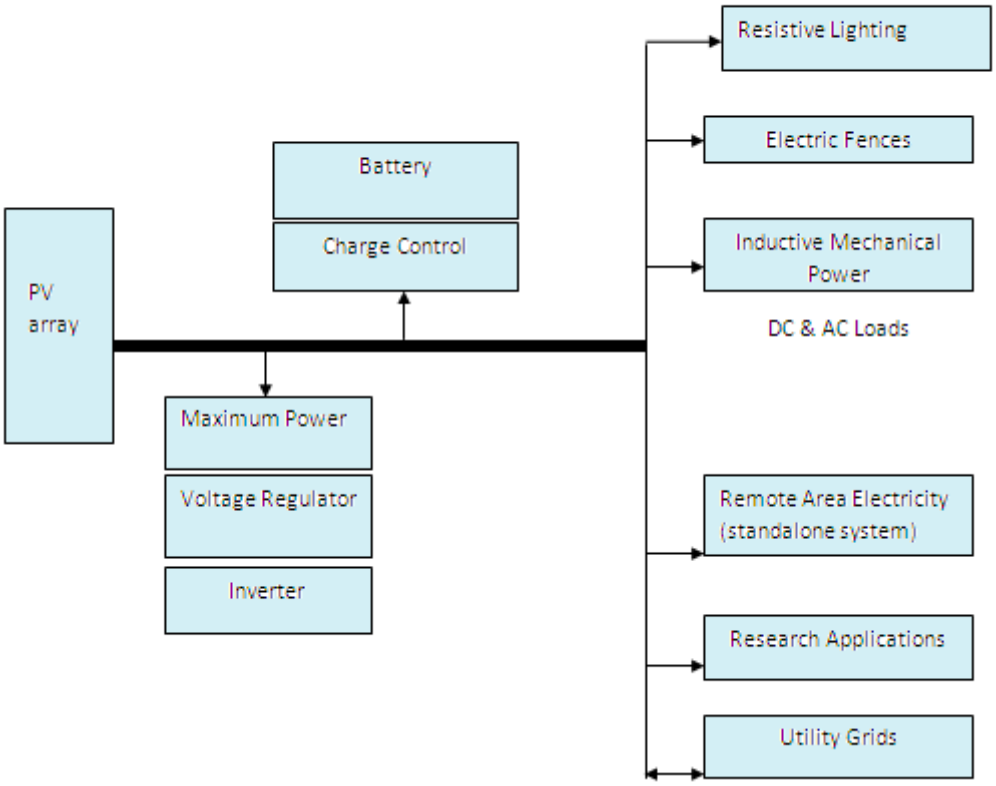


**Fig-1.4 PV System Configuration**

## 1.2 PV SYSTEM CONFIGURATION-

Fig-1.4 shows typical PV system. The system can be distinguished based on several factors like-depending on type of load AC or DC load, depending on utility stand

alone or grid connected. Inverter configuration is mainly used for AC systems. Battery is used to deal with fluctuations. In order to tackle the present day energy crisis and relatively high cost of photovoltaic generator we have to modify the system in a manner such that maximum energy can be extracted from solar radiations. The design of a demand of a motor driven system, connected to a photovoltaic source is that MPPT controller should maximize the energy produced by the module to operate under variable power restrictions. Features such as low cost, and high energy efficiency convertor to enable its development where it is most needed. In this Dissertation work we have thrown light on how the DC (direct current) current produced by the photovoltaic cell or array can be easily utilized to drive different types of electric drives. The simplest and least expensive way to convert solar energy to mechanical energy is to supply a DC motor from photovoltaic generator because they produce DC (direct current). The solar powered DC motors are now-a-days used in running centrifugal pumps. Since power generated by the Photovoltaic cells varies with the intensity of sun's rays falling on the panel, it has to be used for charging the battery and then the battery should be used to run the DC motors. The dc water pump is driven by dc motor drive. The requirement of torque varies with the speed at which the motor is being driven.

Photovoltaic pumps have got high attention because of development and new initiatives in the solar energy sector, mainly in the fields of materials and technology. Photovoltaic pumps driven by motors are running worldwide, but the major problem is that they lack in ease of maintenance due to the presence of commutator and brushes. Due to this reason induction motors driven pumping is considered to be a good option as the reliability and maintenance are taken care of by the use of induction motors. The Photovoltaic panel takes energy from solar radiations and converts it into electricity. This electrical energy is fed through induction motor to the inverter. In IM driven centrifugal pumps output power is directly proportional to the cube of speed of rotor.

Many schemes have come up for controlling the speed of IM among which vector control is most effective method .By using this technique, the induction motor can be made to run and control like a separately excited DC motor. Though this technique gives decoupled control, it requires reference frame transformations, which increases the complexity of the system but gives the fast response.

## 1.3 INTRODUCTION OF ARTIFICIAL INTELLIGENT (AI) TECHNIQUES IN PV SYSTEM

Generally conventional PID controllers do not give proper results for a non linear system, so intelligent control methods find great use for existing non linear system. The DC /AC motors are widely used in all industrial applications, for speed and position control. Accuracy of the controller output is important for process control industry. In real world most of the systems are non linear, so proper tuning of controller will remove much of difficulties like overshoot, delay in settling time and decrease the offset in the system which require expert knowledge and sometimes even not possible with conventional PID controller. So to overcome these difficulties three basic intelligent control techniques are Fuzzy logic, Neural Network and Adaptive neuro-fuzzy interference system (ANFIS).

Present work of design of speed controller for DC/AC motor powered by Photovoltaic source is done on Fuzzy Logic controller and ANFIS controller. Fuzzy controllers design depends on expert knowledge. Here one has to select membership function (based on expert knowledge), form the rule base (based on controller i/p and o/p). After rule base is made generate a Fis file and run the Fuzzy controller. ANFIS is hybrid controller which is combination of fuzzy logic and neural network. It learns the plant automatically, through training of data (i/p and o/p) and creates membership function and rule base accordingly. Thus, it adapts itself according to the plant, and the changes made in the plant automatically. This is major advantage of ANFIS over Fuzzy logic is that expert knowledge (human operator) to tune the plant, by adjusting the membership function is removed.

## 1.4 DISSERTATION OBJECTIVE

This Dissertation work, presents a solar powered DC motor and indirect vector control scheme for solar powered induction motor that can be used in various industrial applications. The main characteristics of the work done in this Dissertation are as follows.

1) The correspondence between the PV generator and two types of motor, the separately excited DC motor and Induction motor, both driving centrifugal pump load are examined so that the maximum amount of mechanical output can be possessed.

2) Atmospheric differentiation performs a major role in power generation from PV module and it makes a difference to the functioning of both DC motor and Induction motor (IM) drive. To achieve this purpose, a Perturb and Observe (P&O) based maximum power point tracking controller is brought to uses as to obtain maximum power from the PV module at different atmospheric circumstances.

3) Modeling of solar panel along with the boost converter is being is done in this Dissertation work, whose switching can be controlled by varying the duty ratio, in accordance with the maximum power tracked by MPPT.

4) Capacity of the controller to practice the maximum switching pulse through HBPWM (hysteresis band pulse width modulation) technique, and indirect vector control of induction motor in which rotor quadrature axis flux is made zero.

5) Artificial Intelligent control techniques Fuzzy and ANFIS have been implemented over conventional PID controller for speed control of DC/AC motor (IM). This makes the system free from mathematical modeling and non- linearity in the system is also considered. Emphasis is also made for getting finer results.

## 1.5 DISSERTATION OUTLINE

The chapter wise description of this dissertation is given as under:

**Chapter-I** gives the introductory view of the overall work that has been presented in this Dissertation. This chapter also gives brief introduction steps of PV system modeling.

**Chapter-II** presents brief literature review modeling of photovoltaic system, modeling of photovoltaic system, and modeling of induction motor drive speed control.

**Chapter-III** discusses the main theory behind the work, system modeling, details of control algorithm have been discussed in detail.

**Chapter-IV** presents speed control of DC motor and induction motor using artificial intelligent (AI) control techniques (Fuzzy and ANFIS).

**Chapter-V** presents the simulation and experimental results.

**Chapter-VI** gives the main conclusion and future scope of the work.

# CHAPTER II

# LITERATURE REVIEW

## 2.1 GENERAL

From the available literature, it is revealed that photovoltaic module can easily modeled with separately excited DC motor and Induction motor, the use of specific MPPT(Maximum power point tracking)controllers has been used for enhancing the output power of the module which effects the performance the drive for a specific application. Induction motor control using vector control (FOC) method is a more efficient and faster technique than scalar control as it is based on decoupling effect which shows self-governing control on torque and flux of the motor, as a result motor response becomes fast as compared to scalar control. PI controller is used for speed control of DC motor. This heuristic method can improve the operational reliability and sturdiness of the closed loop system over the traditional controllers. Research has proved that a Vector control scheme is lot better than scalar control as far as closed loop system is designed.

The major drawback of vector control (FOC) is the complexity involved in designing the controller. During the past few years several approaches for developing converters that show high efficiency and minimum loss. Inverters and boost converter used are having minimum switching losses. Dedicated simulation software like MATLAB with Simulink has made the modeling and simulation of the system efficient and simple. The advancement in the speed control techniques from a basic proportional control to vector control, and other intelligent control like fuzzy and ANFIS etc. have resulted in a remarkable improvement in the response of the drive.

## 2.2 LITERATURE REVIEW

### 2.2.1 Modeling of photovoltaic system

The complete Dissertation work can be sub divided into three works-Modeling of photovoltaic system, modeling of DC motor speed control and modeling of Induction motor drive speed control. The existing literature survey available on modeling of photovoltaic System is also categorized under three sections-modeling of photovoltaic module, Maximum power tracking controller and boost converter which is well described in the following works-

**Samer Alsadi et al. -** done modeling on MSX-50 solar module, the modeling equations are briefly discussed for a solar cell. The flowchart explaining how to implement Perturb and Observe method is also discussed in his work [1]. The expressions for calculating of inductance and capacitance of boost converter.

**N.Pandiarajan et al. –** described step by step mathematical modeling of Photovoltaic Module with Simulink, [2] which helps to have better viewpoint of I-V and P-V curve.

**M.Abdulkadir et al.-** analyzed electrical circuit model of PV panel it can be seen that solar output current depends mainly on solar irradiation, it also has discussed that Photovoltaic voltage is the function of junction voltage across the diode [3] which is basic characteristic of the semiconductor.

**Kinal Kachhiya et al. –**analyzed BP SX 150S solar module simulation in Matlab for different values of solar insulation. The characteristic equations of PV module implemented in Matlab Simulink are well seen [4] Incremental Conductance method is used to calculate Pmax which shows fairly good results. Thus proposed simulation model along with MPPT model canbe used with DC-DC boost converter to obtain required DC voltage.

**Tarak Salmi et al.–** discussed on a Matlab/Simulink model of PV cell. He has also discussed briefly the effect of varying Temperature, effect of varying series resistance of

the cell Rs, effect of varying shunt resistance Rsh and effect of varying Is [5]. He has also discussed how PV cells can be connected to form module and then array.

**Patil Sahebrao N.et al. –**presents complete model of the PV system containing solar PV cell, DC-DC converter and MPPT control using Incremental Conductance method is simulated in Matlab[6]. The modeled DC-DC buck boost converter along with MPPT can be used as a reference for implementation of actual system. PWM signal generation is also discussed, that is used to control the duty cycle of converter.

**Biji.G. -**presents modeling and simulation of pump system using photovoltaic source for maximum efficiency. His work deals with calculation of chopping ratio for maximum power operation of array [7]. The whole system modeling is described briefly; buy showing calculation of each section.

**Johan H.R. Enslin et al.-**presents MPPTs' integrated in PV panels this has led to great reduction in cost of MPPTs and increased efficiency making it adorable for used in small photovoltaic systems[8]. The integrated MPPT is a simple controller using soft switching technique.

**A.S.Samosir et al.-**presents modeling of solar photovoltaic module 100W under various operating conditions the proposed MPPT shows how it can track even in sudden changes of loading and environmental conditions [9].Simulink model of Incremental Conductance along with integral regulator is used.

**E.Skoplaki et al.-** discussed PV efficiency as a function of operating temperature of photovoltaic module (one sun commercial grade silicon-based solar cells/modules) [10].The efficiency and the output power of the photovoltaic is inversely proportional on the operating temperature.

**C.Liu et al.-** discussed earlier the use of MPPT has successfully led to decrease per unit cost of output power generated from photovoltaic module. This work has led to new

method for MPPT control estimate-perturb–perturb (EPP),this perturb process conducts search over extremely nonlinear PV characteristics, and estimate process compensates the perturb process for radiance variation [11]. The principles of operation of perturb and observe (P&O), modified perturb and observe (MP&O) and estimate-perturb-perturb (EPP) have been discussed briefly.

**T.J. McMohan et al. –** presents the work was done on effect of light intensity on electron collection of Photovoltaic cells. It shows that current is diminished in thin film cells under intense solar radiation due to increased recombination [12].

**Guanghui Li et al. –**presents the novel controller used that was able to track the sun position and adjusting the load. Improved perturb and observe (IP&O) method is used as it overcomes the drawbacks of P&O method [13] like- oscillation around MPP in steady state, slow response speed, and cannot track properly under rapid changing environment .

**Karl H. Edelmoser et al.** – presents DC-DC/ DC-AC converter is used for converting solar power produced to AC system, which reduces the size of topologies comparatively [14]. The losses are also reduced to great extent.

### 2.2.2 Literature Review on DC Motor drives and their control-

**Mohan Kashyap et al.** – presents simple modeling techniques for photovoltaic powered PMDC motor [15]. It was a simple modeling of DC motor but this modeling has given insight how DC motor can be used for modeling along with photovoltaic cell.

**Ziyad M. Saiamch et al.**– presents PV powered volumetric water pump which is again a PMDC motor, but Electrical array reconfiguration controller (EARC) presents a new approach to optimize the performance of PV pumps [16]. The approach produces sufficient staring current to start the motor even at low irradiance. This has led to increase in pumping ours of solar cell.

**J.Appelbaum et al.** – have discussed the transient and steady state characteristics of DC motor solar powered [17]. Simple boost converter is used for stepping up the DC voltage level.

**S.M Alghuwainen et al.** – presents the steady state characteristics of DC motor supplied from photovoltaic cell, it is concluded that separately excited DC motor with centrifugal pump as load is best suited for matching to photovoltaic generators [18].

**P.C.Sen et al.** – The book best elaborates DC drives, with different types of power converters. Different type of DC drives used for specific purposes are discussed in this book [19].

**M.M Saied et al. –** deals how modeling can be done for best matching of solar array with DC motors [20]. Voltage current plane best describes the motor characteristics assuming perfect match for all radiation level.

**S.Singer et al. -** presents solar powered DC motor starting current characteristics verses torque ratio with and without MPPT [21]. The result shows centrifugal pump best matches with PV source, and constant load matches the worse.

**S.M. Alghuwainem-** Photovoltaic powered Dc motor drives are used for driving different types of load; it can also be used for driving self-excited 3-phase Induction motor [22]. Dc chopper is used to achieve maximum efficiency from PV array by varying the field current of DC motor.

### 2.2.3 Literature Review on Induction Motor drives and their control techniques-

**M. Rama Prasad Reddy et al. –**hysteresis controller is presented for vector control of induction motor. 6-sector Algorithm is developed with takes in account of both direct torque control and field oriented control [23]. It gives good dynamic response, which reduces total harmonic distortion (THD**).**

**Adel Aktaibi et al. –** presents the dynamic modeling of induction motor, using dq axis transformation of stator and rotor variables in the arbitrary frame [24]. Two motors one of 3hp and other of 2250 hp are simulated and the machine parameters are described in the paper.

**Ashutosh Mishra et al. –**presents indirect vector control scheme of Induction motor using fuzzy logic controller and PI controller. Hysteresis current regulator is used in which motor actual 3-phase currents are compared with reference currents [25].

**N.Ravi Shankar Reddy et al. –**presents an algorithm which minimizes the switching loss for vector control of induction motor [26]. FOC has led to fast transient response, which is like separately excited DC motor.

**Gilberto C.D. Sousa et al. -**presents work that deals with indirect vector controlled of solar boat induction motor drive for speed and torque control of the motor using fuzzy logic control for optimizing the efficiency [27].

**Aurbinda Panda et al. –**work shows that water pumps powered by photovoltaic source are widely used find large applications these days. The PV source operates at MPP (Maximum power point), output of which is given to DC converter and then fed for direct torque control of induction motor [28].

**M. Arrouf et al.–**presents work on solar fed vector control of induction motor. And results are seen at different solar radiation and temperature, which shows torque and dq components of current changes but its average value remains the same [29].

**J.A. Santiago Gonzalez et al. –** presents single solar panel driven three phase induction motor. Perturb and observe method of MPPT is implemented [30]. The panel delivers rated

210W, and open loop speed is obtained. All the equations are well described in the work, and PWM signal is generated by pulse width modulation technique.

**Olorunfemi Ojo –** presents photovoltaic fed induction motor using current controlled inverter [31]. The transient and steady state characteristics of induction motor are limited by the chopping ratio of the DC converter.

**B.N. Singh et al –** presents induction motor fed by photovoltaic source for isolated pumping system. MMPT has also been applied for extracting the maximum power, .and driver system has been proposed for extracting maximum efficiency [32].

**A Abbou et al. –** presents modeling and d space implementation of induction control using constant volts /hertz (V/f) principle. A great variety of variable speed drives are used today are mainly V/f control drive [33]. The V/f control is mainly based on steady state characteristics of induction motor.

**N.K. Lujara et al.** – presents both DC and AC motor drives feed from induction motor. For different insolation level different heads of water is pumped, but the model helps in maximizing the efficiency of pumping head [34]. The efficiency of model is calculated at very critical parameters of system and losses are estimated.

**I.H Altas et al.–**presents electrical system powered by photovoltaic cell, the generated power shows great fluctuation due to environmental conditions**.** So design of the controller is made by extra caution, using fuzzy logic controller (FLC) [35].

**R.C Zowaraka et al. –** discussed mainly to study the performance of induction motor with inverter supply [36]. The inverter switching is done by PWM (pulse width modulation), technique.

**P.Ragot et al. –** presented on, new optimization software Pro@Design which models and optimizes brushless DC motor for solar airplane. The crucial part of the calculation is no of motors that is to be used in the plane [37]. If the parameter is changed new optimal solution can be found quickly**.**

**Hiroaki Yamamoto et al.** – presents method of auto tuning based on indirect vector control. The auto tuning method based on rotor flux is implemented for giving torque command [38]. This takes into account stator core loss, of induction motor which appears in transient voltage waveform.

**K. Naga Sujatha et al. –**presented work on new speed control approach based on the Adaptive Neuro-Fuzzy Inference System (ANFIS) to a closed-loop, variable speed induction motor (IM) drive [39].

**B. Venkata Ranganadha et al. –**presents work on hysteresis controller, applied in non-linear model. It is compared with conventional PWM controller and found that it is more efficient [40]. The THD (total harmonic distortion) is also comparatively reduced.

**Nelson Mendez Gomez et al. –**presents work on single panel photovoltaic system for running three phase induction motor and cost efficiency is also maintained. DC output of boost converter is converted to three phase 180 conduction mode three level inverter [41]. The speed control is also achieved by Atmega 328.

**Vongmanee V et al. –**work shows water pumps powered by photovoltaic source are widely used find large applications these days[42]. The PV source operates at MPP (Maximum power point), output of which is given to DC converter and then fed to indirect vector control scheme, for independent flux and torque control of induction motor.

**A.M. Sharaf et al. –**work was mainly on Photovoltaic powered electric vehicle. Controller performance is gauged for both constant speed and variable speed drive [43]. Since the

motor used is PMDC (permanent magnet DC) motor so DC-DC is used for maintaining the required voltage profile.

**Joshua Anzicek et al. -**work discusses design of DC-DC boost converter and control system for hybrid vehicles. Mosfet is used as a switch, having a high efficiency of 98% [44].The Design equations were well established by the results.

**Ulrich Herrmann et al. –**present optimal control of DC to AC converter, fed by photovoltaic source so as to use in residential applications [45]**.**

### 2.2.4 Literature Review on Artificial Intelligent Techniques on speed control of DC motor and induction motor –

**B.A.A Omar et al.** –presents speed control of separately excited DC motor using ANFIS controller [46]. The performance is compared with PID controller and improved response speed with lesser ripples in output is achieved.

**Rekha Kushwah et al.** –presents speed control using Fuzzy logic and PID controller for DC motor in Matlab/ Simulink [47]. The results shows an improved setting time, overshoot and control performance with the use of fuzzy logic controller.

**R.P. Sudhakar et al. -** discusses the enhanced performance of DC motor using Fuzzy logic controller. The results showed that it outperformed the conventional PID controller. The comparison of PID controller and Fuzzy controller was also studied [48].

**Rasoul Rahmani et al.–**discusses optimized Fuzzy logic controller using particle swarm optimization for DC motor speed control using Matlab/ Simulink [49]. Also presents comparative study of performance of PID controller, fuzzy logic controller and optimized fuzzy logic controller.

**Philip A. Adewuyie -** discusses that both PID and Fuzzy logic controllers can be used to get the speed control of DC motor. The work shows that PID traces the output response well and gives much overshoot; Fuzzy controller decreases the overshoot but makes the response sluggish [50]. So a compromise has to be made depending on application of motor.

**Salim jyoti et al. –**presents design of fuzzy logic controller for speed control of DC motor in lab view. The work explains how Fuzzy controller is used, making of rule base and de-fuzzification process [51].

**Atul Kumar Dewangan et al.** – presents model description of separately excited DC motor and description of fuzzy logic controller design for creating membership function [52].The paper shows proper designing a fuzzy logic controller shows far better results than conventional PID controller.

## 2.3 CONCLUSION

This literature review provides a basic knowledge of the area. It provides a knowledge about types of control algorithms already implemented in past, there advantages, disadvantages, etc. this review provides a knowledge about what are those parameters which can be controlled to provide better performance of the system. For an example consider FOC (field oriented control) theory. This method helps to control the torque and flux of induction motor independently. This makes the system response faster, than the traditional scalar control. Other algorithms which are implemented for tracking maximum power from the photovoltaic panel like P&O (perturb and observe) and Incremental conductance method papers have been reviewed.

Apart from this works on intelligent control techniques Fuzzy and ANFIS applied to separately excited DC motor and induction motor for speed control have been reviewed.

# CHAPTER III

# MODELLING OF SOLAR POWERED ELECTRIC DRIVES

## 3.1 GENERAL

Solar powered electric drives are now days are boon in industrial as well as remote area applications like pumping, lighting etc. The fossil fuels are now becoming extinct, which has lead to emergence of renewable sector especially photovoltaic in the economy. They require solar energy as input which is free of cost and also available in plenty. Modeling of electric drives along with their speed control is performed using Matlab Simulink. The results of the modeling discussed later in Chapter V and comparison is done on different control techniques.

## 3.2 The modeling of solar powered electric (AC and DC) drives –

The modeling is carried out in following steps of simple modeling-

1. Modeling of Photovoltaic cell, module and panel.
2. Modeling of MPPT controller.
3. Designing of BOOST converter.
4. Modeling of separately excited DC motor with water pump as load.
5. Inverter configuration and HBPWM generation.
6. Modeling of Induction motor.
7. Control and estimation of Induction motor drives.

Here we are going to discuss the modeling of all of all the sections briefly-

### 3.2.1 Modeling of Photovoltaic system-

Photovoltaic system models have been in great transition for researchers and professionals, and form an considerable part of electrical power generation. Single diode circuit model is the most common model used to predict energy production in photovoltaic cell modeling. The typical PV cell consist of light generated current source (Isc) in parallel with single diode as shown in Fig.3.1

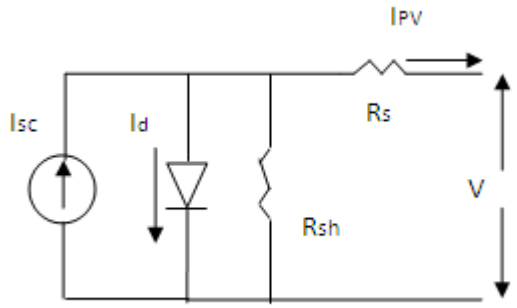


**Fig-3.1 Photovoltaic cell model using single diode**

The output current equation $I_{PV}$ of photovoltaic cell is given as-

$$\mathbf{I_{PV} = I_{SC} - I_d.} \qquad \mathbf{(3.1)}$$

The model included temperature dependent photocurrent Isc and the saturation current of the diode Id.

$$\mathbf{I_{PV} = I_{sc} - I_d\left[e^{\frac{q(V+IRs)}{nkT}} - 1\right]} \qquad \mathbf{(3.2)}$$

The photovoltaic current is irradiance and temperature dependent so the PV current is measured at some given reference conditions. Therefore, reference temperature is taken asT1 and nominal radiation is G (nom).

$$\mathbf{I_{sc} = I_L(T1) + K_0(T - T1)} \qquad \mathbf{(3.3)}$$

$$\mathbf{I_{sc} = I_{SC}(T1, nom)\frac{G}{G(nom)}} \quad (3.4)$$

$$\mathbf{K_0 = \frac{I_{sc}(T2) - I_{sc}(T1)}{(T2 - T1)}} \quad (3.5)$$

$$\mathbf{I_d = I_d(T1) * (\frac{T1}{T2})\wedge \frac{3}{n} e^{\frac{qV_q(T1)}{nk(\frac{1}{T1}-\frac{1}{T2})}}} \quad (3.6)$$

And reverse saturation current is given by Id (T1)-

$$\mathbf{I_d(T1) = \frac{I_{SC}(T1)}{e^{\frac{qV_{0C}(T1)}{nkT1}} - 1}} \quad (3.7)$$

A series resistance Rs was included; which represents the resistance inside each cell in the connection between cells.

$$\boldsymbol{R_s = -\frac{dV}{dI_{V_{0C}}} - \frac{1}{X_v}} \quad (3.8)$$

$$\boldsymbol{X_V = I_0(T1)\frac{q}{nkT1} e^{\frac{qV_{0C}(T1)}{nkT1}} - \frac{1}{X_V}} \quad (3.9)$$

**PV module**- A PV module is interconnection of several cells in series and in parallel combination in order to form a module of described power and voltage level. The basic equation of output current of the Photovoltaic module IPV of a single diode model is explained by equation-

$$\mathbf{I_{PV} = N_p I_{sc} - N_s I_d \left\{ exp\left( \frac{q(V_{PV} + I_{PV} R_s)}{N_s KAT} \right) - 1 \right\} - V_{PV+} \left( \frac{I_{PV} R_s}{R_p} \right)} \quad (3.10)$$

These reference values are generally provided by manufacturers of PV modules for specified operating conditions such as at STC (Standard Test Conditions) for which the irradiance is 1000 W/m^2and cell temperature is $25^0$C. Real operating conditions are always different from standard conditions. Based on above equations and using electrical specifications in Table1 the PV system modeling has been done using Matlab Simulink as shown in Fig3.2.

**PV Array**- PV Array is formed by interconnection of different solar modules of same or different ratings in series and parallel. In order to get benefits from modeling of photovoltaic module explained above, an array of 3 PV modules were inter connected in series and all of them are connected to the external control block. This connection was done to drive loads of higher power ratings.

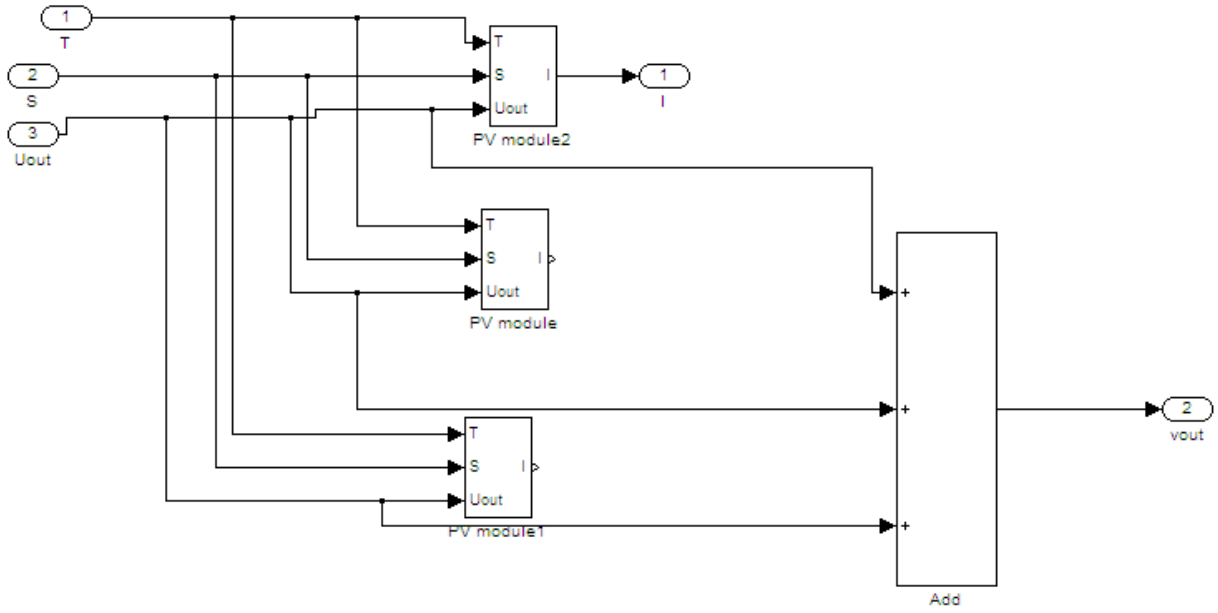


**Fig3.2. PV Module and PV Array**

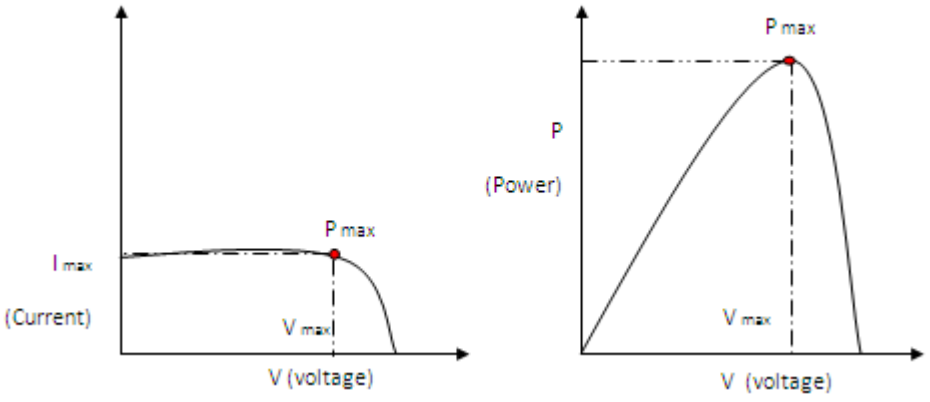


**Fig.3.3 I-V and P-V curves of Photovoltaic module respectively**

The Photovoltaic and I-V curves of a photovoltaic module are reliant to a high degree on the exposure to sun's radiation. The exposure to sun's radiation remains in a flux due to changes in environmental factors, but control mechanisms that can identify such changes are present and can change the working of the solar panel so that the much needed load demands are met. Greater is the solar irradiation; greater would be the solar input to the photovoltaic panel thus raising the power size for the same voltage amount. The increase in the solar irradiation level leads to increase in the open circuit voltage $V_{oc}$. The reason attributed to this increase as a matter of fact is of sunlight happening to fall on to the solar cell, there is a provision of greater amount of excitation energy to the electrons, which in turn increases the movement of electrons as a result of which more power is generated.

### 3.2.2 Modeling of MPPT controller-

PV modules are semiconductor device that are capable of directly changing the form of solar radiations into electrical energy. On the I-V curve of photovoltaic system there is MPP (maximum power point) which without fail occurs at the knee of the curve where the maximum PV is obtained as shown in Fig.3. A variety of maximum power point tracking (MPPT) algorithm are brought to existence. The algorithms differ in implementation complications, convergence, sensed parameters, speed cost, and range of operation, popularity and their usage. Most of the maximum power point tracking (MPPT) algorithms tries to find out the maximum power point (MPP) by comparing the output power of PV module before and after MPP, posterior to which duty cycle of the converter is changed on its basis. In this report, MPPT is achieved through Perturb and Observe method.

In this algorithm a trivial disturbance is brought into the system. Resulting from this disturbance the power of PV module fluctuates continuously. The perturbation if causes the power to increase, it is carried on in the same direction. When the maximum power is achieved, the power decreases at the next instant and thus the disturbance is reversed henceforth. When an even state is achieved the algorithm wavers around the peak

point. To keep lesser differentiation in power, the magnitude of disturbance introduced is to be kept absolutely small as shown in Fig.3.4.

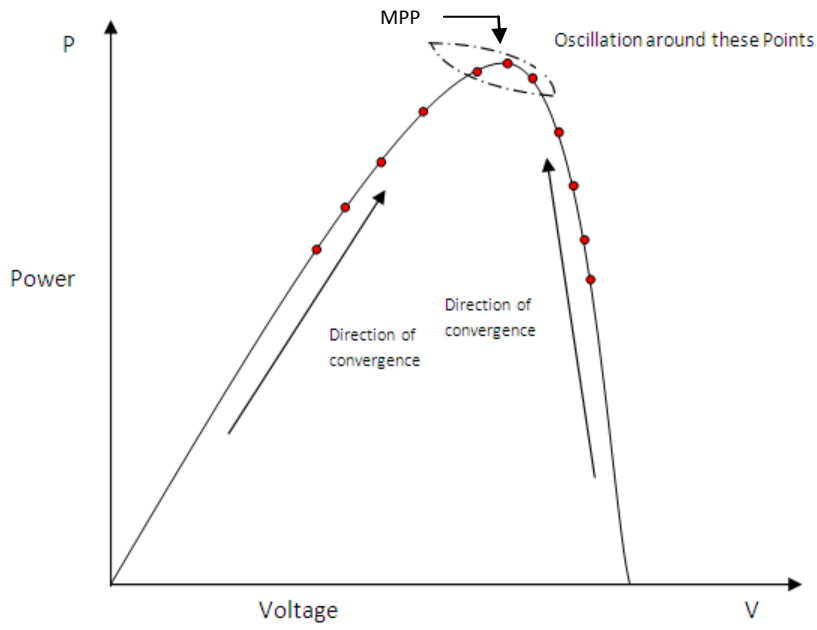


**Fig.3.4 Perturb and Observe Algorithm**

Figure.3.5 shows the flow chart of the algorithm. The current and voltage value is read by the algorithm from the PV module. Further, the calculation of power is done from the measured voltage and current. The numerical value of voltage and power at $k_{th}$ time are noted. Once more the subsequent value of voltage and current at $(k+1)_{th}$ instant are measured and power is calculated from the measured value. The power and the voltage values at the latter instant is subtracted with the values at the former. Through observation of the power voltage curve of the PV module we notice that in the right hand side curve where the voltage is approximately constant, there is a negative slope of power ($dP/dV<0$). Contrary to this, the left hand side the slope is positive ($dP/dV>0$). The right hand side curve indicates the smaller value duty cycle (nearer to zero) whereas left hand side is for the greater duty cycle (nearer to unity). Depending on the sign of dP(P(k+1)-P(k)) and dV (V(k+1)- V(k)) after subtraction the algorithm decides if the duty cycle needs to be increased or rather decreased.

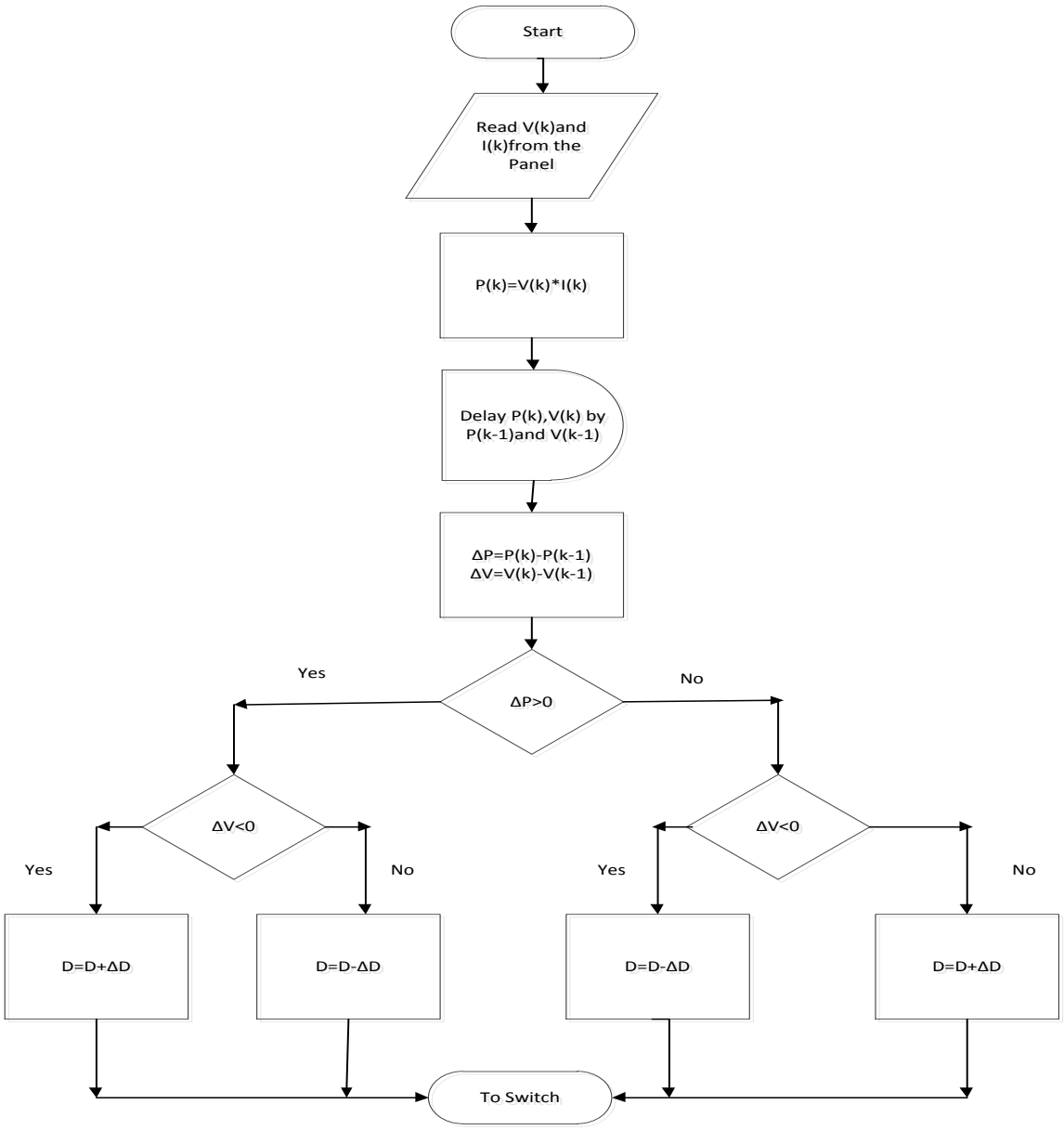


**Fig.3.5 Flowchart of Perturb and Observe Algorithm**

**Limitations-**In a condition of rapid flux in irradiation, the MPP shifts to the right hand side of the curve as well. As per the algorithm, the change has taken place due to disturbance caused and in the next instance it alters the direction of perturbation thus moving away from MPP as shown in the figure. As a matter of fact, a single sensor namely the voltage sensor, in this algorithm in order to sense the PV array voltage, thus reducing the cost of implementation and making its implementation feasible. The time complications involved

in this algorithm is quiet low but on reaching a nearer position to the MPP, it does not stop at the MPP and keeps on perturbing in both the directions. When such a situation occurs, the algorithm has reached quiet near to the MPP and now we can get an optimum error limit or instead can use a wait function which further increases the time complexity of the algorithm.The detailed Simulink model of MPPT controller is shown in Fig.3.6. The Vpv and Ipv are taken as the input to MPPT unit, duty cycle D is obtained as output. In this small perturbation of .001 is introduced.

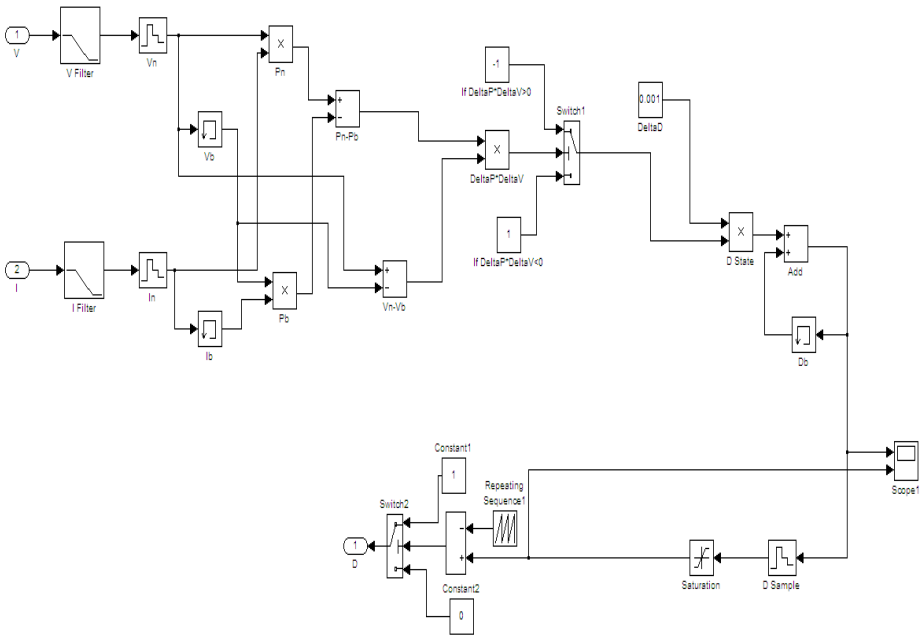


**Fig.3.6 Simulink Model of MPPT Controller**

### 3.2.3 Design of Boost Converter

The three fundamental converter configurations are buck, boost and buck-boost. A Boost Converter as shown in Fig. 3.7 is an on/off device that takes a dc voltage at one level and converts it to higher voltage level. The fig.8 shows basic configuration of converter where the switch is Power Mosfet, other components of boost converter is inductor, diode and capacitor. Considering the fact that the output of the converter is reliant on the position of the Mosfet switch, the converters are regulated by duty cycle which is

decided by the MPPT controller senses, the current atmospheric condition and produces favorable duty cycle. By altering the duty cycle, it is possible to achieve the most favorable load resistance for the PV module.

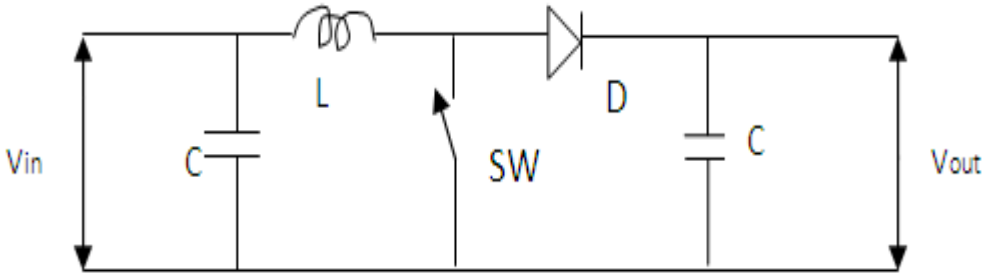


**Fig.3.7. Simple Boost Converter**

### 3.2.3.1 Modes of Operation

The modes of operation of boost converter can well be classified under 2 heads: the charging mode and discharging mode.

**Charging Mode**- When the switch is closed and the induction is charged by source through switch, the boost converter is said to be operating under the charging mode. The diode restrains the flow of current from the source to the load and the demand of the load is met by the discharging of the capacitor.

**Discharging Mode**- In this mode the switch is open and diode is forward biased, the inductor now discharges and together with the source charges the capacitor and meets the load demand.

### 3.2.3.2 Necessary Calculation for Design of Boost Converter

- **Calculation the Maximum switch current**

The initial step in calculation of the switch current is to ascertain the **duty cycle D**, for the minimum input voltage. The rationale behind using the minimum input voltage is that it leads to maximum switch current.

$$\mathbf{D=1-\frac{V_{in}*\eta}{V_{out}}} \quad \textbf{(3.11)}$$

The second step in estimating the maximum switch current is to as curtailment of the inductor ripple current.

$$\mathbf{\Delta I_L = \frac{V_{in(min)}*D}{f_s*L}} \quad \textbf{(3.12)}$$

$$\mathbf{I_{out(max)} = \left(I_{lim(min)-\frac{\Delta I_L}{2}}\right) * (1 - D)} \quad \textbf{(3.13)}$$

$$\mathbf{I_{SW(max)} = \frac{\Delta I_L}{2} + \frac{I_{out(max)}}{1-D}} \quad \textbf{(3.14)}$$

- **Inductor Selection-**

Now range of inductor value can be determined from the below equations (5) and (6)-

$$\mathbf{L = \frac{V_{in}*(V_{out}-V_{in})}{\Delta I_L * f_s * V_{out}}} \quad \textbf{(3.15)}$$

$$\mathbf{\Delta I_L = (0.2 \text{ to } 0.4) * I_{out(max)} * \frac{V_{out}}{V_{in}}} \quad \textbf{(3.16)}$$

- **Rectifier Diode Selection-**

Rectifier diode selection is based on following equations-

$$\mathbf{I_f = I_{out(max)}} \quad \textbf{(3.17)}$$

- **Input capacitor selection-**

It is important to make the incoming voltage stable because of peak current requirement of a switching power supply. It would be excellent if low equivalent series resistance (ESR) ceramic capacitors can be used as input capacitors.

- **Output Capacitor selection-**

The minimum output capacitor value can be adjusted with following equations for the expected output voltage ripple.

$$\mathbf{C_{out}} = \frac{\mathbf{I_{out(max)} * D}}{\mathbf{f_s * \Delta V_{out}}} \quad \textbf{(3.18)}$$

The ripple current was defined to assure a small oscillation around MPP. The bus voltage was defined using the minimum required voltage for the selected inverter configuration and PWM strategy-

$$\mathbf{V_{bus} > V_{rms} * 1.414} \quad \textbf{(3.19)}$$

The K gain necessary for the converter can be calculated using:

$$\mathbf{K > (V_{rms} * 1.414)/V_{mpp.max}} \quad \textbf{(3.20)}$$

The detailed Simulink model of boost circuit is shown in Fig.3.8

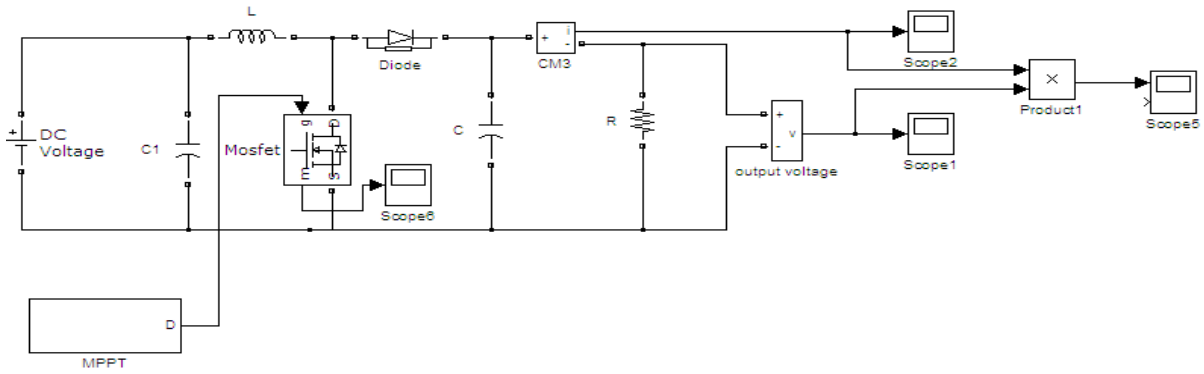


**Fig.3.8 Boost Converter circuit in Simulink**

### 3.2.4 DC Motor Model for Pumping Load

Some of the many necessary features that should be possessed by DC motors include cheapness, reliability, durability, high efficiency, and low operation voltage. DC motors can directly be aligned with a PV module. Brushed types are comparatively cheaper and more common in spite of the fact that brushes need periodic replacement. The speed control of a DC motor connected to PV module can be easily understood. DC motor can be

broadly classified as series, shunt and separately excited DC motor. Here separately excited DC motor is only discussed as it is best used for pumping application. The circuit design of a separately excited DC motor is shown in Fig3.9.

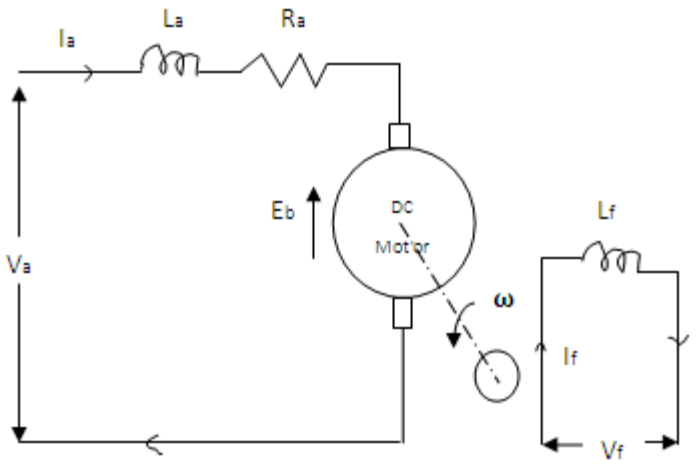


**Fig.3.9 Schematic of separately excited DC Motor**

A shunt type of DC motor can be wired as separately excited DC motor by connecting field and armature circuits with two separate sources. With the help of separately excited DC system, electrical power supplied by voltage source is transformed into mechanical output to rotor through magnetic coupling. The armature coil of the DC motor can be represented by an inductance ($L_a$) in series with resistance ($R_a$) and with a series induced voltage ($E_b$), which is in opposition with the voltage source ($V_a$). A separate equation for the equivalent circuit can be derived by using Kirchhoff's voltage law around the electrical loop.

$$\mathbf{V_a(k) = R_a I_a(k) + L_a \frac{dI_a(k)}{dt} + E_b(k)} \qquad \mathbf{(3.21)}$$

Where

- $E_b(k) = K_e \omega_m(k)$
- if = constant; therefore $K_e = K_T$

The total torque of the motor must be equal zero therefore,

$$\mathbf{T_e(k) - J\frac{d\omega_m(k)}{dt} - B\omega_m(k) - T_L(k) = 0} \quad \textbf{(3.22)}$$

The electromagnetic torque ($T_e$) produced is directly proportional to the motor armature winding and can be written as –

$$\mathbf{T_e = K_T * i_a} \quad \textbf{(3.23)}$$

The load torque is given by

$$\mathbf{T_L = K_0 + K_1\omega_m + K_2\omega_m} \quad \textbf{(3.24)}$$

### 3.2.5 Water Pumping Systems and Photovoltaic Power

The working of a water pumping system requires a power source. Usually, AC powered system is economic and does not require much maintenance when AC power is used from the nearby power grid. However, in many rural areas, water sources are spread over many miles of land and power lines are less. Putting of a new transmission line and a transformer to the location is at most times undesirably costly. Windmill share been put up conventionally in such areas; many of them are, however, out of function due to improper maintenance and age. These days, internal combustion engines are used by many standalone type water pumping systems use internal combustion engines. These systems are easy to carry and install. But, they possess a number of drawbacks. One of them is that they need frequent site visits for refueling and repair purposes. The other one being that diesel fuel is costly at most of the times and not easily available in rural areas of many developing countries. PV systems are mostly used and have greater reliability because of their lowest life cycle cost, mainly for usage in cases where less than 10KW is needed, where grid electricity is unavailable and where the heavy cost factor of engines make it impossible to function.

Usually, 2 kinds of pumps are used for water-pumping applications. One being positive displacement pump and the other being is centrifugal pump. In displacement pumps, the water output and the speed of the pump are in direct proportion, but mostly not reliant on head. These pumps are applied for solar water pumping from lower head to higher head. Centrifugal pumps lined up with solar panels are used for low-head **ρ**applications. Centrifugal pumps are made for fixed-head usages, and there is a relative increase in the pressure difference produced with the speed of the pump. Centrifugal pumps also have comparatively high efficiency and are able to pump a high volume of water. Because of the given benefits centrifugal pump is used for our project work. Any pump is featured by its absorptive power which is of course a mechanical power produced by the shaft coupled with pump, which is given by equation:

$$\mathbf{P = \rho gHQ/\eta} \qquad \textbf{(3.25)}$$

The useful power is:

$$\mathbf{Pu = \rho gHQ} \qquad \textbf{(3.26)}$$

The ratio of power drawn by the motor to the power used by the pump to lift a given quantity of water at a specified pumping rate and head is known as the "wire to water efficiency".

$$\mathbf{H = \frac{\rho gQH}{P_{in}}} \qquad \textbf{(3.27)}$$

Where $\mathbf{P_{in} = V_a * I_a}$ **(3.28)**

Pump Type- **CENTRIFUGAL PUMP MODEL**

Rated Torque- $\mathbf{T_p = 0.001\omega\text{^}1.8}$

### 3.2.6 Block Diagram of the DC System

Figure3.10 shows the block diagram of DC motor drive powered by PV panel. PID controller is being tuned for no load and on load conditions and the control action is being performed maintaining a constant speed of 1500 rpm.

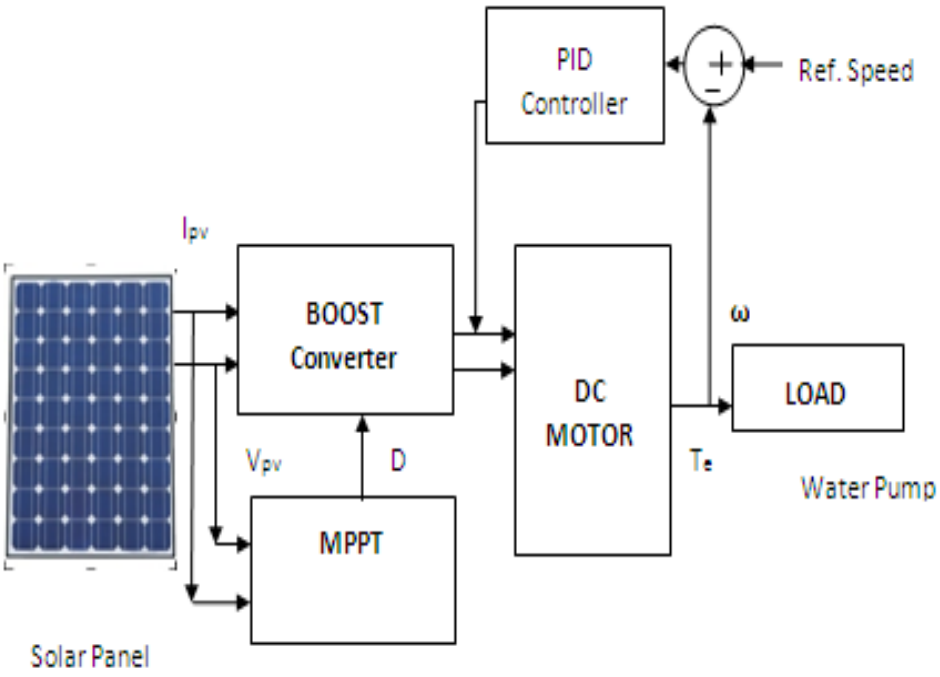


**Fig.3.10 Block Diagram of the DC System**

### 3.2.7 Three Phase Inverter Configuration

The DC-AC converter is usually called inverter or voltage fed converters. The device functions by taking a DC voltage and transforming it into AC voltage at a specific frequency. The frequency of output relies completely on the frequency of power electronic switches like transistor, Mosfet, IGBT etc. Fundamentally, there are two categories of inverter: single phase inverter and three phase inverter. The quality of converter is based on the THD (Total harmonic Distortion) and its efficiency. The three phase inverter used to carry out this dissertation is using IGBT type switches and the switching technique of hysteresis band current-controlled PWM (HBPWM) inverter. The IGBT inverter is built by using six IGBT blocks. The DC link input voltage is represented by VDC voltage source.

Three phase bridge inverters are widely used for ac motor drives and general purpose ac supplies. The induction motor is sourced by a voltage-controlled PWM inverter

that is made by applying a Universal Bridge block. The circuit consists of three half-bridges, which are mutually phase shifted by $120^0$to generate three phase voltage waves.

### 3.2.8 HYSTERISIS BAND CURRENT CONTROL PWM (HBPWM)

There are several types of PWM techniques Sinusoidal PWM (SPWM),Selected harmonic elimination(SHE) PWM, Minimum ripple current PWM, Space vector PWM, Hysteresis band current control PWM(HBPWM),Sinusoidal PWM with instantaneous current control, Sigma-delta modulation .The hysteresis band current control PWM has been used as it can be used easily, with fast transient response, direct controlling of device peak current and practical unawareness of dc link voltage ripple that allows a lower filter capacitor.

The HBPWM is originally a spontaneous feedback current control method of PWM wherein the real current continually examines the command current within a given hysteresis band. The Fig.3.11 elucidates the operation principle of HBPWM for a half bridge inverter.

The controller generates the sinusoidal current wave as reference wave of required amplitude and frequency, and it is put in comparison with the actual phase current wave. As the current rises over a specified hysteresis band, the upper switch in the half-bridge is turned off and the lower switch is turned on. As a result the output voltage transitions from +0.5Vd to -0.5Vd, and the current starts to decay. As the current crosses the lower band limit, the lower switch is turned off and the upper switch is turned on. The actual current wave is thus compelled to follow the sine reference wave within the hysteresis band by back- and-forth switching of the upper and lower switches.

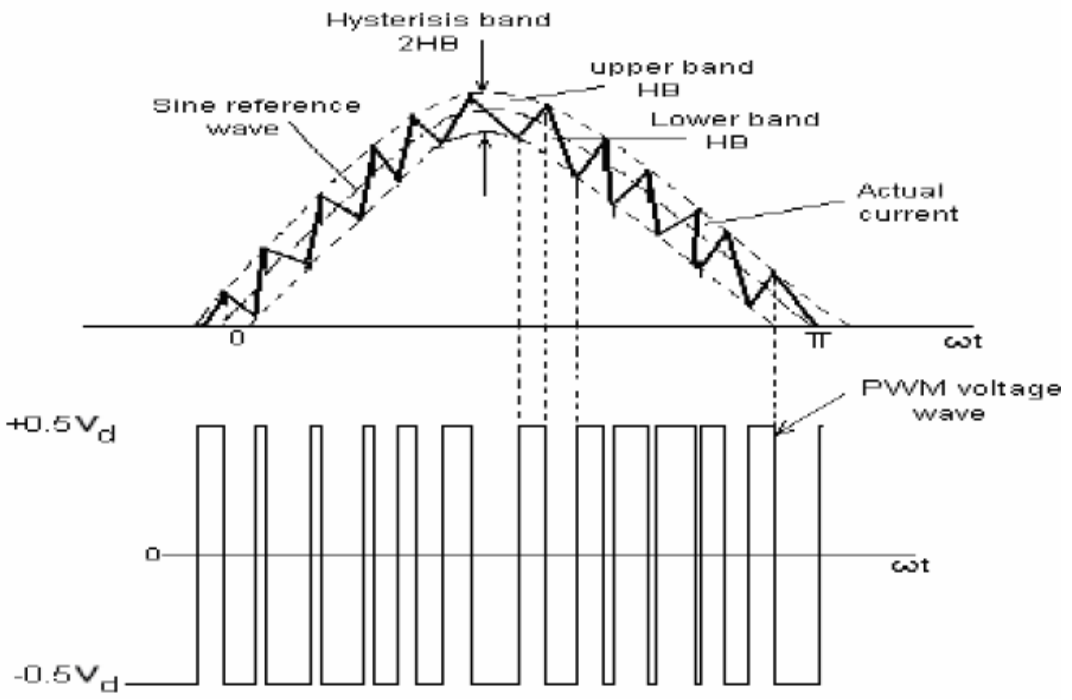


**Fig. 3.11 PWM generation by HBPWM controller**

Thus, the inverter necessarily is rendered as a mode current having peak to peak current ripple, which is regulated within the hysteresis band in spite of Vd fluctuation. The peak-to peak current ripple and the switching frequency are related to the width of the hysteresis band. The HBPWM inverter control method is shown in the Fig 3.12. The supply to the HBPWM controller is three phase current errors and the outputs are the switching patterns to the PWM inverter. K in the figure stands for the normalization factor and is applied in the purpose of scaling the current error input to the HBPWM controller.

The hysteresis current controller (HBPWM) gives output pulses to the inverter according to this rule.

$\left|I_{m,ref} - i_m\right| < \varepsilon$ keep the output pulse at the same state $i_{m,ref} - i_m > \varepsilon$ let output pulse=1(high).

$I_{m,ref} - i_m < \varepsilon$ let output pulse =0(low),Where m=a, b, c phases and ε is the hysteresis band.

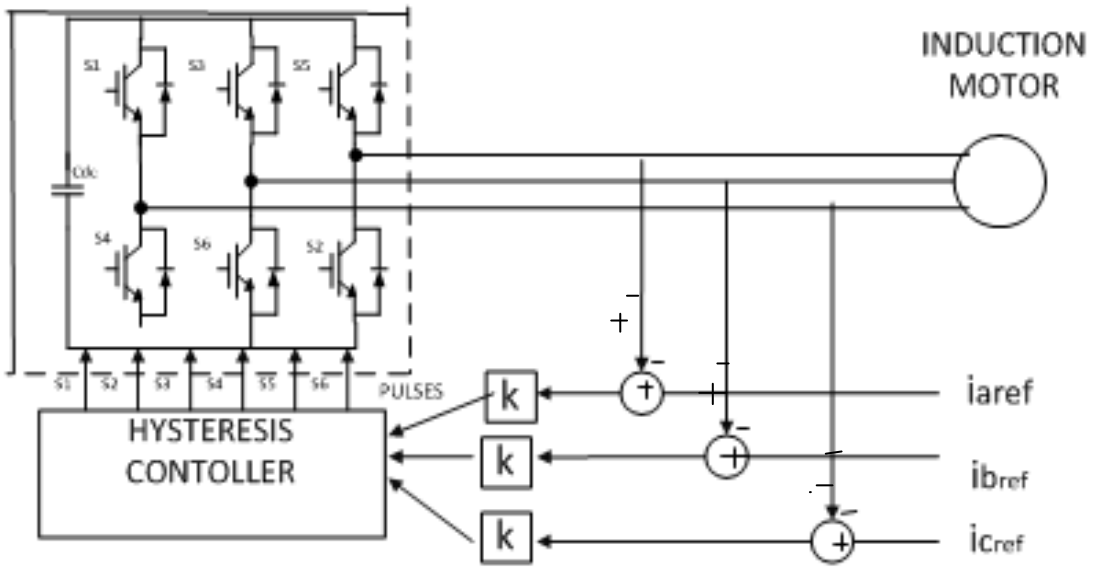


**Fig. 3.12 Schematic Diagram of Hysteresis Controller in Inverter loop**

The algorithm for this is:

$i_{m,ref}(t) = I_{m,ref} \sin(\omega t)$

Upper band $i_u = i_{m,ref}(t) + \Delta$

Lower band $i_l = i_{m,ref}(t) - \Delta$

If $i_m > i_u$, $V_{mo} = -\frac{V_{dc}}{2}$

If $i_m < i_L$, $V_{mo} = \frac{V_{dc}}{2}$

Else, maintain the same state. Where m=a, b, c phases is load current and Vdc is the dc link voltage of the inverter.

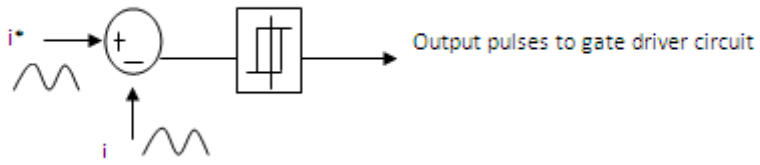


**Fig. 3.13 control scheme of HBPWM**

The main disadvantage of this method is that the PWM frequency is inconsistent and, as a result non optimum harmonics will occur.

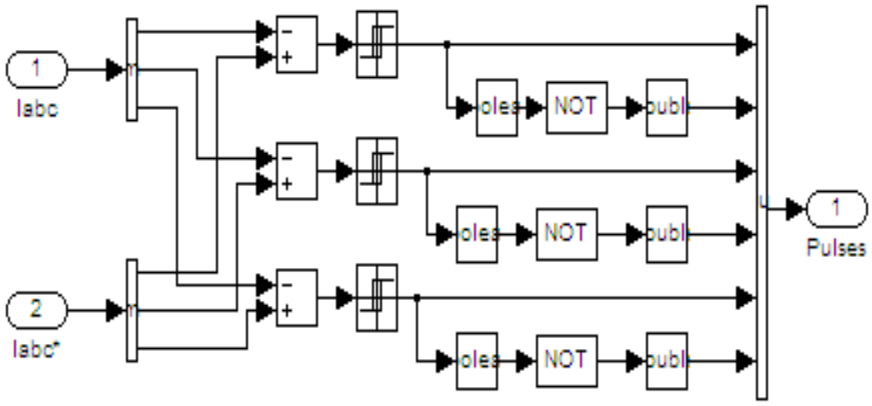


**Fig3.14. Simulink Diagram of 3-ϕ HBPWM Controller**

### 3.2.9 Three Phase Induction Motor

Induction motor (IM) is most commonly used in industry. These machines are very economical, rugged and reliable and available in ranges of fractional horse power (FHP).One of the most fundamental principles of induction machine are creation of a rotating and sinusoidally distributed magnetic field in the air gap. Basically the machine can be looked upon as three phase transformer with rotating and short-circuited secondary. During no load the motor rotates at almost synchronous speed, when the load is applied the rotor speed decreases in relation to synchronous speed. Here 0.5 Hp motor is use for simulation. In an adjustable-speed drive, the machine normally constitutes the element within a feedback loop, therefore its transient behavior is taken into consideration. Also high performance drive control like vector control is based on dynamic d-q model of machine, thus a good understanding of d-q model is necessary. Thus a three phase induction machine can be represented as two phase machine using Parks' transformation.

### 3.2.10 Indirect Vector Control Strategy Used in Induction Motor Drives-

The various control strategy can be broadly classified as under-

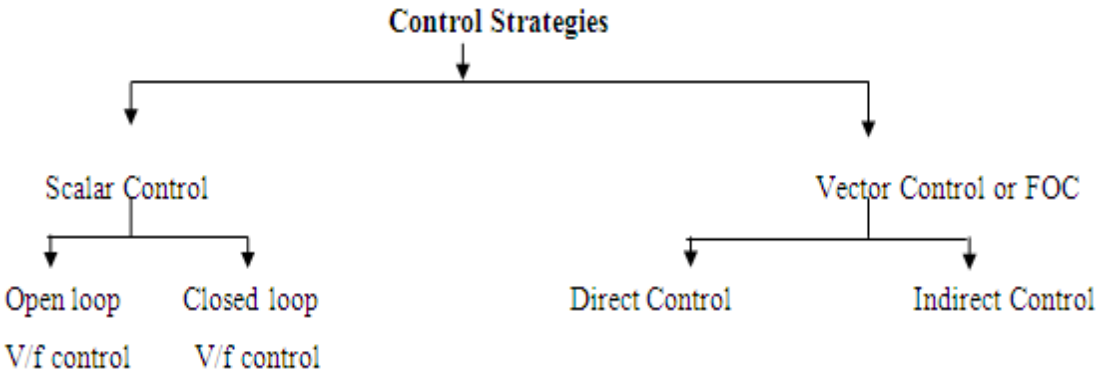


**Fig.3.15 Flowchart of control strategies**

In this work, we have only to deal with Indirect Vector Control or Rotor Flux Oriented Control of induction motor. In motor drives a mechanical load featured by inertia J, friction coefficient B, and load torque T. The speed control loop uses a proportional-integral controller to generate the quadrature-axis current reference iq* that regulates the motor torque. The motor flux is regulated by the direct-axis current reference id*. Block DQ-ABC is required to change id* and iq* into current references ia*, ib*, and ic* for the current regulator. Power and Voltage Measurement blocks exhibit signals for the objective of visualization. Motor current, speed, and torque signals are present at the output of the 'Asynchronous Machine' block. The behavior of the induction machine subjected to rotor-flux-oriented control is same as that of the separately excited DC machine.

Synchronously rotating axis $d^e$-$q^e$ are rotating ahead of $d^r$-$q^r$ axis by the positive slip angle $\theta_{sl}$ corresponding to slip frequency $\boldsymbol{\omega}_{sl}$. The space angle of the rotor flux space phasor ($\theta_e$) is achieved as the aggregate of the rotor angle ($\theta_r$) and the reference value of the slip angle ($\theta_{sl}$).

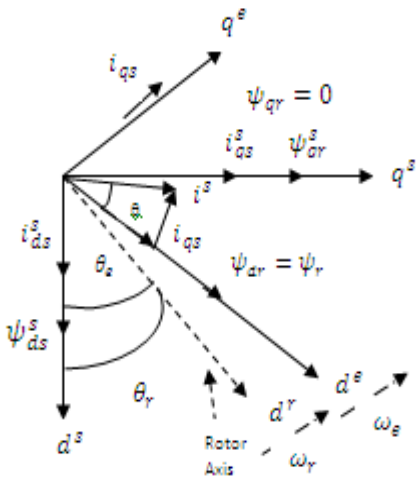


**Fig.3.16 Phasor Diagram of indirect vector control**

$$\boldsymbol{\theta_e = \int \omega_e \, dt = \int (\omega_r + \omega_{sl}) dt = \theta_r + \theta_{sl}} \qquad \textbf{(3.29)}$$

In indirect vector control method, the unit vector signals (cosθe and sinθe) are produced in feed forward manner. The $d^e$-$q^e$ equivalent circuit of induction motoris used because all the sinusoidal quantities used in stationary frame become dc in synchronous frame. Now, derivation of control equations of indirect vector control with help of $d^e$-$q^e$ equivalent circuits. The rotor circuit equation

$$\frac{\mathbf{d\psi_{dr}}}{\mathbf{dt}} + \mathbf{R_r i_{dr}} - (\boldsymbol{\omega_e - \omega_r}) \qquad \textbf{(3.30)}$$

$$\frac{\mathbf{d\psi_{qr}}}{\mathbf{dt}} + \mathbf{R_r i_{qr}} + (\boldsymbol{\omega_e - \omega_r})\boldsymbol{\psi_{dr}} \qquad \textbf{(3.31)}$$

The rotor flux linkage expression can be given as-

$$\boldsymbol{\psi_{dr} = L_r i_{dr} + L_m i_{ds}} \qquad \textbf{(3.32)}$$

$$\boldsymbol{\psi_{qr} = L_r i_{qr} + L_m i_{qs}} \qquad \textbf{(3.33)}$$

From above equation we can write-

$$\boldsymbol{i_{dr} = \frac{1}{L_r}\psi_{dr} - \frac{L_m}{L_r} i_{ds}} \quad \textbf{(3.34)}$$

$$\boldsymbol{i_{qr} = \frac{1}{L_r}\psi_{qr} - \frac{L_m}{L_r} i_{qs}} \quad \textbf{(3.35)}$$

Now rotor current in equation (3.30) & (5.31) can be eliminated from equation (3.34) & (3.35).

$$\boldsymbol{\frac{d\psi_{dr}}{dt} + \frac{R_r}{L_r}\psi_{dr} - \frac{L_m}{L_r} R_r i_{ds} - \omega_{sl}\psi_{qr} = 0} \quad \textbf{(3.36)}$$

$$\boldsymbol{\frac{d\psi_{qr}}{dt} + \frac{R_r}{L_r}\psi_{qr} - \frac{L_m}{L_r} R_r i_{qs} - \omega_{sl}\psi_{dr} = 0} \quad \textbf{(3.37)}$$

Where $\omega_{sl} = \omega_e - \omega_r$ has been eliminated.

For decoupling control, it is desirable that

$$\boldsymbol{\psi_{qr}=0} \quad \textbf{(3.38)}$$

That is, $\boldsymbol{\frac{d\psi_{qr}}{dt} = 0}$ **(3.39)**

So that total rotor flux is directed towards $d^e$-$q^e$ axis, $\psi_{dr} = \psi_r$

Substituting the above conditions in equation (3.36) & (3.37)

$$\boldsymbol{\frac{L_r}{R_r}\frac{d\psi_r}{dt} + \psi_r = L_m i_{ds}} \quad \textbf{(3.40)}$$

$$\boldsymbol{\omega_{sl} = \frac{L_m R_r}{\psi_r L_r} i_{qs}} \quad \textbf{(3.41)}$$

If rotor flux $\psi_r$ =constant, then

$$\boldsymbol{\psi_r = L_m i_{ds}} \quad \textbf{(3.42)}$$

In other words, the rotor flux is directly proportional to current $i_{ds}$ in steady state. The power circuit consists of PWM inverter, A hysteresis band current control PWM is shown, The speed regulator loop produces the torque components of current $i_{qs}*$, as usual. The flux component of current $i_{ds}$*for desired rotor flux $\psi_r$. The variation of magnetizing inductance $L_m$ will cause some drift in the flux. The slip frequency $\omega_{sl}$ is generated from $i_{qs}*$in feed forward manner, which is added to $\omega_r$ to generate frequency signal $\omega_e$. The unit vector cosθ and sinθ are generated from $\omega_e$ by integration.

In order to convert the two rotating input quantities into two stationary output quantities, we need to work out the inverse Park transformations –

$$\begin{vmatrix} i_{sa} \\ i_{sb} \end{vmatrix} = \begin{vmatrix} \cos\theta & -\sin\theta \\ \sin\theta & \cos\theta \end{vmatrix} \begin{vmatrix} i_{sd} \\ i_{sq} \end{vmatrix} \quad \textbf{(3.43)}$$

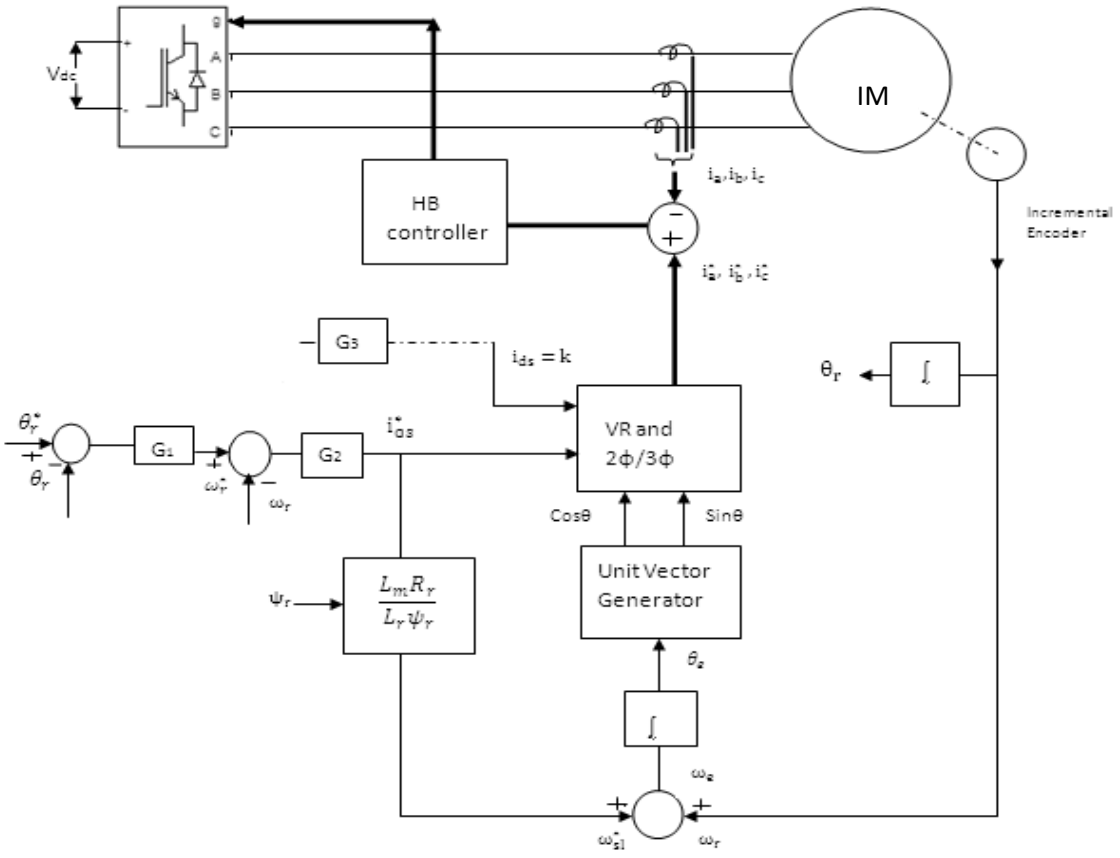


**Fig.3.17 Block diagram of Vector Control strategy**

From the diagram shown in Fig 3.17 it is clear that motor torque and flux have independent control. The torque is controlled by controlling the current $i_a$, and the flux is not affected and we get the fast transient response and high toque/ratio with the rated flux.

### 3.2.11 Block diagram of indirect vector control of induction motor

Fig.3.18 presents the overall block diagram of the proposed solar powered indirect vector controlled induction motor drive. Here the 3-phase induction motor is sourced by a PV module through a DC-DC converter and an inverter. Perturb and Observe method of tracking MPP (maximum power point) has been applied to extract the maximum power from the PV module. In this Dissertation HBPWM controller along with vector control scheme using PID controller is used to enhance the performance dynamics of the whole system.

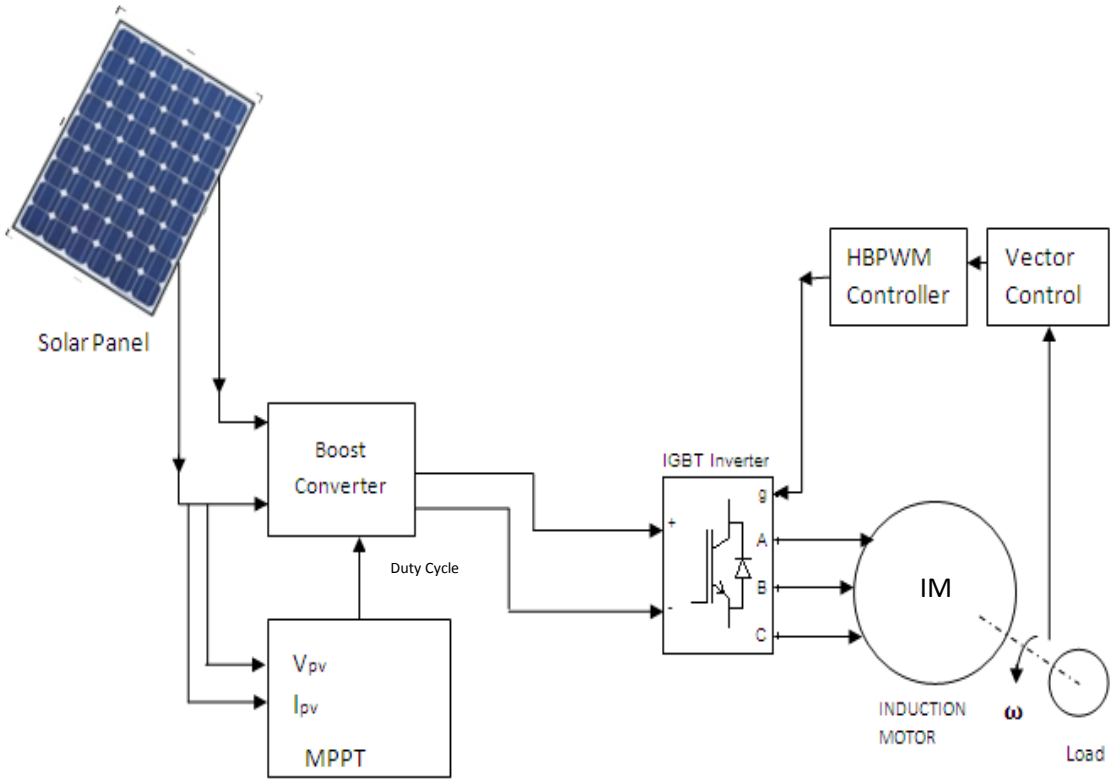


**Fig.3.18 Block Diagram of Photovoltaic powered Induction Motor Drive**

## 3.3 CONCLUSION

Modeling of different sections is discussed in detail. All the modeling work is being carried out in Matlab Simulink. Control algorithms for MPPT controller, is designed successfully and with the help of boost converter so that the desired output voltage can be generated. DC motor and induction motor using centrifugal pump as load is used in drives configuration for pumping applications. After results have been obtained by tuning PI controller different artificial techniques have been applied which is discussed in next chapter.

# CHAPTER IV

# ARTIFICIAL INTELLIGENT TECHNIQUES IN PV SYSTEM

## 4.1 GENERAL

Most of the system in present world are non linear, for this the use of conventional PID controller are not suitable as they increases the overshoot, settling time and the control action performed is not so appropriate. Therefore new control technique known as Artificial Intelligence (AI) is proposed for non linear system. Among the various Artificial Intelligent techniques **FUZZY LOGIC, NEURAL NETWORK** and **ADAPTIVE NEURO-FUZZY INFERENCE SYSTEM (ANFIS)** are the important one. In this Dissertation, Fuzzy and ANFIS controllers are used over the conventional PID controller for speed control of DC and induction motor which do not require any mathematical modeling of the non-linear system.

## 4.2 FUZZY LOGIC CONTROLLER (FLC)

Based on way of human thinking, Lotfi Zadeh, developed fuzzy logic or fuzzy set theory. Fuzzy Logic (FL) unlike Boolean logic deals with problems that have fuzziness or vagueness. The general methodology of reasoning in FL is by "IF…THEN…" statements or rules. In this chapter, discussion is done on principles of FL and its application in speed control of electric drive system. A fuzzy inference system consists of mapping from a given input set to an output set using FL, as shown in Fig.4.1.so that on the basis of which inference and conclusion can be made. The fuzzy inference process consist of following five steps-

- Fuzzification of input variables
- Application of fuzzy operator (AND, OR, NOT) in the IF (antecedent) part of the rule.
- Implication from the antecedent to consequent (THEN part of the rule).

- Aggregation of the consequents across the rules.
- Defuzzification

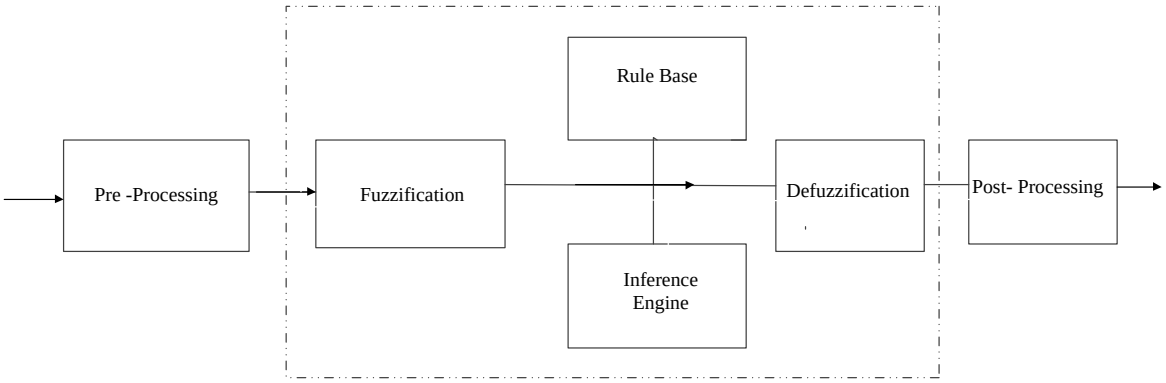


**Fig.4.1 Basic Block Diagram of Fuzzy logic controller**

### 4.2.1 Speed Control Application

Now, consider the fuzzy speed controller block as shown in Fig4.2 in speed control of DC motor and in a vector controlled induction motor drive system. The controller observes the pattern of speed loop error signal (e), $e = \omega^* - \omega$ and corresponding updated the output signal so that the actual speed (**ω**) matches the reference speed ($\omega^*$) i.e 1500 rpm.

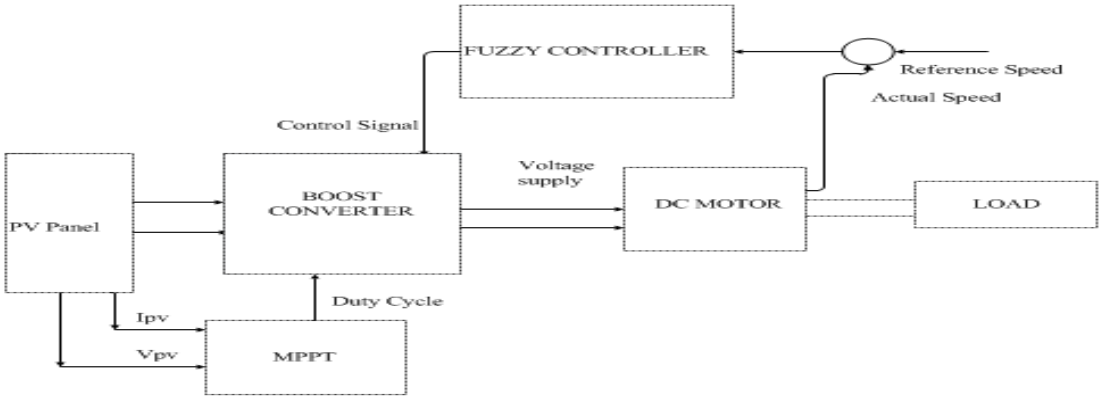


**Fig4.2 Block Diagram of DC Motor Control Using Fuzzy Logic Controller**

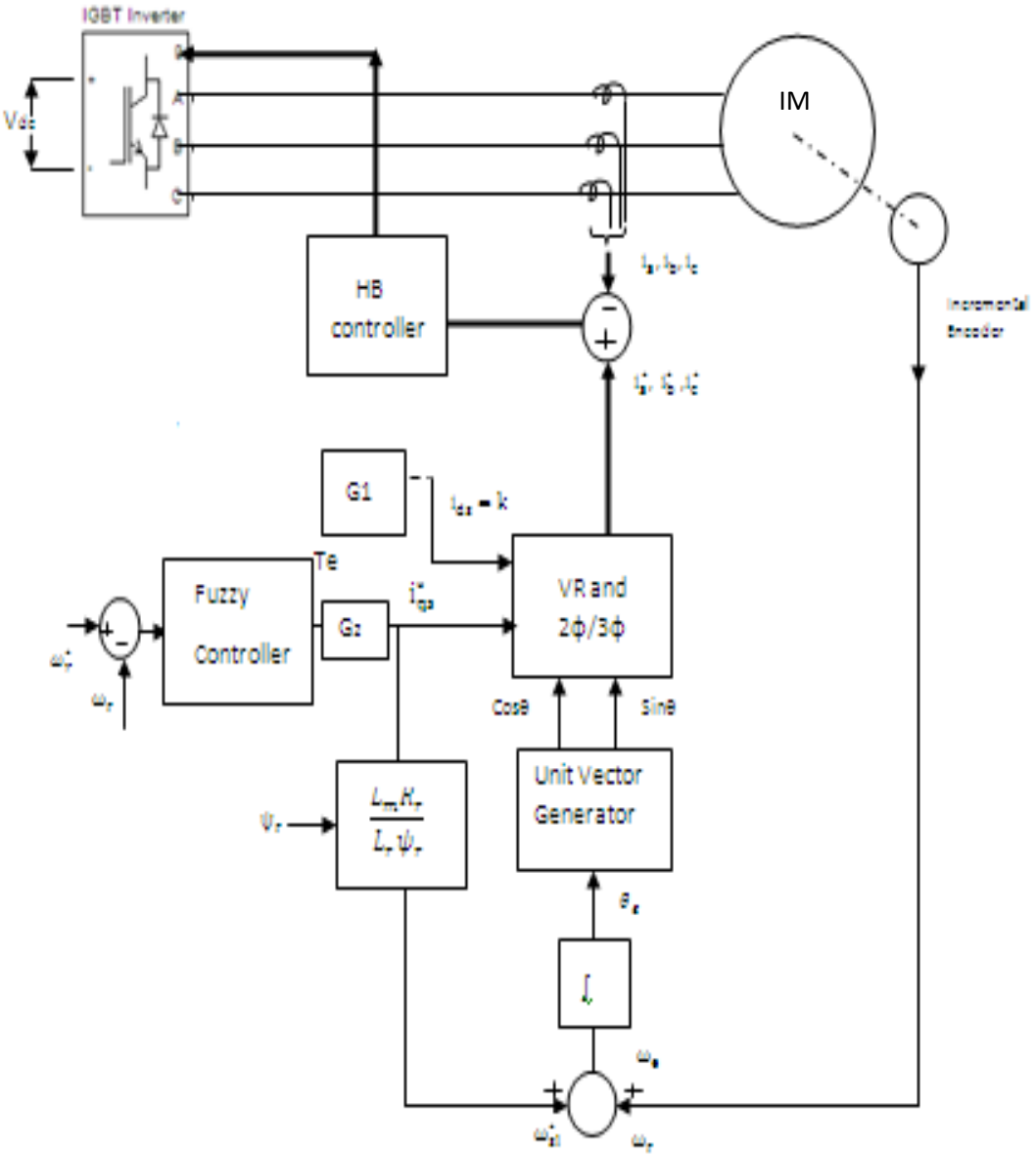


**Fig.4.3 Block Diagram of IM control using FLC.**

The PID controller in both the systems DC and AC is replaced with fuzzy controller block in MATLAB SIMULINK. The fuzzy logic controller is designed using fuzzy logic toolbox. The FIS file (Mamdani) is created; different membership function values and shape are chosen for both input and output. The Rule base is created after those using linguistic variables, and the implication of rules is done through Mamdani type.

#### 4.2.1.1Membership Function

**DC System-** Seven triangular shaped membership function having different linguistic term as shown in Fig4.4 (a) is taken in input as well as in output. The range of input is set seeing the speed error range; similarly the range of output is set according to the required output DC voltage.

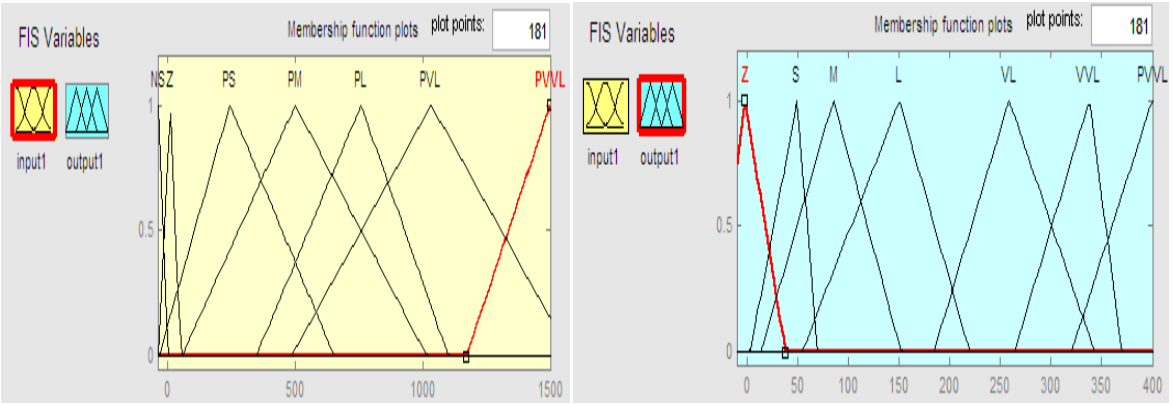


**(a)** **(b)**

**Fig4.4 (a) Input Membership Function(b)Output Membership Function of DC System**

Here different linguistic terms used in input are NS,Z,PS,PM,PL,PVL and PVVL. Similarly different linguistic terms used in output are Z,S,M,L,VL,VVL,PVVL. These linguistic terms have different meanings listed in abbreviations at the starting.

**AC System-**The vector control of photovoltaic powered induction motor drive is performed using fuzzy logic controller. Five triangular shaped membership function are taken in input and output. The different linguistic terms attached to input are Z,S,M,L and VL which is same as output linguistic terms.

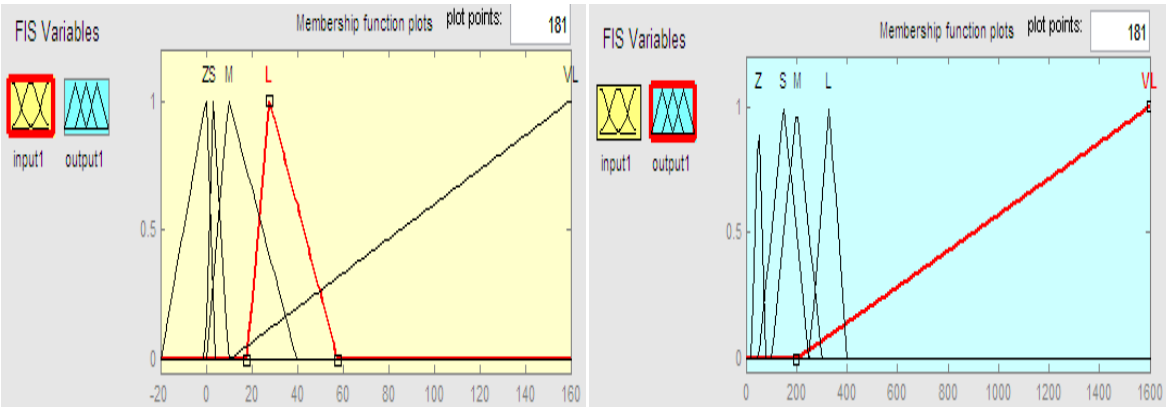


(a) (b)

**Fig4.5(a)Input Membership Function(b)Output Membership Function for AC System**

### 4.2.1.2 Rule Base

Different rule base are made according to the desired output of controller using IF..THEN… rule. The rule base table of both DC and AC system are shown in Table 4.1(a) & (b).

| **I/p (e)** | NS | Z | PS | PM | PL | PVL | PVVL |
|---|---|---|---|---|---|---|---|
| **O/p(v)** | VVL | VVL | VVL | VL | VL | M | Z |
| | PVVL | PVVL | PVVL | VVL | L | L | S |

**(a)**

| **I/p(e)** | Z | S | M | L | VL |
|---|---|---|---|---|---|
| **O/p(T)** | Z | S | M | L | VL |

**(b)**

**Table4.1(a) Rule Table for DC motor (b) Rule Table for Induction motor.**

#### 4.2.1.3 Defuzzification

The results of the implication and aggregation steps are the fuzzy output, which is union of all the outputs of individual rules that are validated or "fired". Conversion of fuzzy output to crisp output is called defuzzification. Few important methods of defuzzification are-

- Center of Area (COA) method
- Height method
- Mean of Maxima method
- Sugeno method

The error signal (e) is generated in case of DC motor by comparing the output speed with the reference speed. The output control signal of the controller is voltage signal (v) which is given back to the DC motor. In case of induction motor vector control of speed is done so the speed error signal (e) is used to generate the torque (T) as control signal which is used to control $i_{qs}$ current of the motor.

## 4.3 Adaptive Neuro-Fuzzy Inference System (ANFIS)

In ANFIS, as the name indicates fuzzy inference system is designed using neural network design method. This means that if the desired input/output data patterns are available for fuzzy system, the MFs and rule table of the fuzzy model can be designed using the neural network training method. Usually Surgeno method is widely used in ANFIS. Suppose X and Y are input variables and F is the defuzzified output signal, and A1, A2, B1 and B2 are triangular membership function and f1, f2 are the output singleton membership function as shown in Fig A typical architecture of an ANFIS is shown in Fig. 5, in which a circle indicates a fixed node, whereas a square indicates an adaptive node. Then rules can be as-

- IF X is A1 AND Y is B1 THEN Z=f1.
- IF X is A2 AND Y is B2 THEN Z=f2.

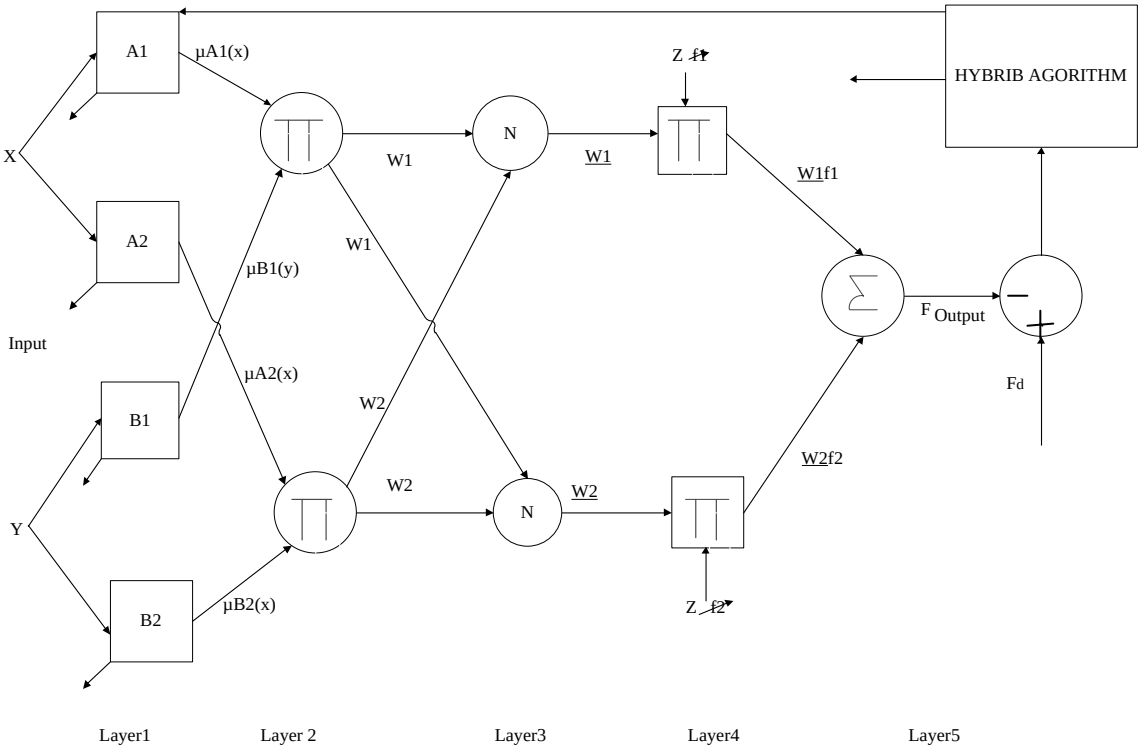


**Fig4.6 ANFIS Structure**

The output F can be constructed as-

$$\mathbf{F}=\frac{w1}{w1+w2}f1+\frac{w2}{w1+w2}f2 \qquad \textbf{(4.1)}$$

The five layers of feed forward neural network are as follows-

- Layer1- Generate the membership grades, μA1(x), μA2(x), μB1(y) and μB2(y).
- Layer2- Generate firing strength by multiplying or AND operation. W1, W2.
- Layer3- Normalize the firing strength. W1, W2.
- Layer4- Calculate the rule output by multiplying with consequent parameters. W1.f1& W2.f2.
- Layer5- Sum of all components output F.

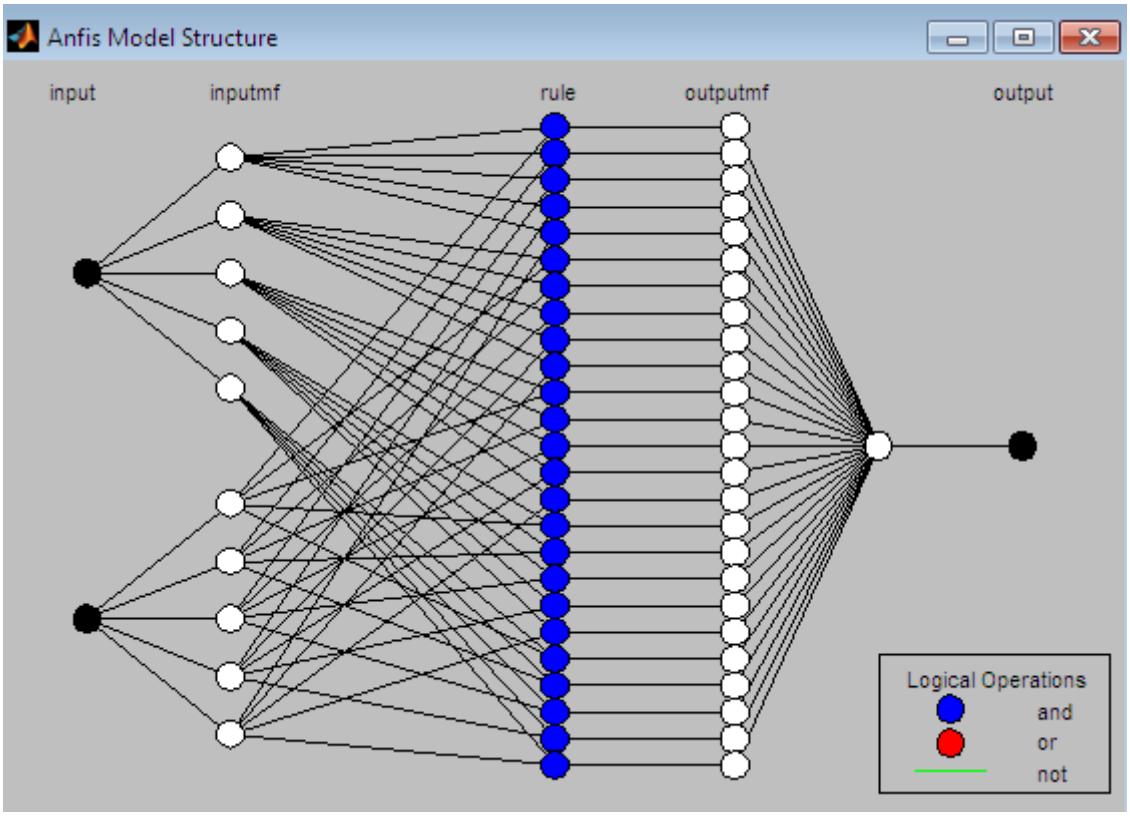


**Fig4.7 ANFIS Structure formed in MATLAB Toolbox.**

The fuzzy controllers shown in Fig 4.2 and Fig.4.3 have been replaced with ANFIS controller and the results were obtained for this controller.

## 4.4 CONCLUSION

This chapter brings insight knowledge of different intelligent controllers used now-a- days in control applications. The working methodology of FUZZY and ANFIS controllers have been discussed in detail, along with their use in speed control in both the motors.

# CHAPTER V

# RESULTS AND DISCUSSIONS

## 5.1 GENERAL

In this chapter result of the various simulations in MATLAB/Simulink and their relevance is discussed. The simulation is carried out in different parts- simulation of solar module, simulation of solar powered DC motor with and without load and simulation solar powered vector control of speed of induction motor drive with and without loading conditions. Apart from this AI techniques fuzzy and ANFIS are also applied to the models and their comparisons are also done.

## 5.2 Simulation Result of Solar PV Module

From the Simulation several results were obtained, the P-V and I-V curve of the panel shown in fig-5.1 and fig-5.2 where obtained which shows readings corresponding to a particular value of solar radiation and temperature. i.e.at 400 irradiances and25 degree Celsius temperature

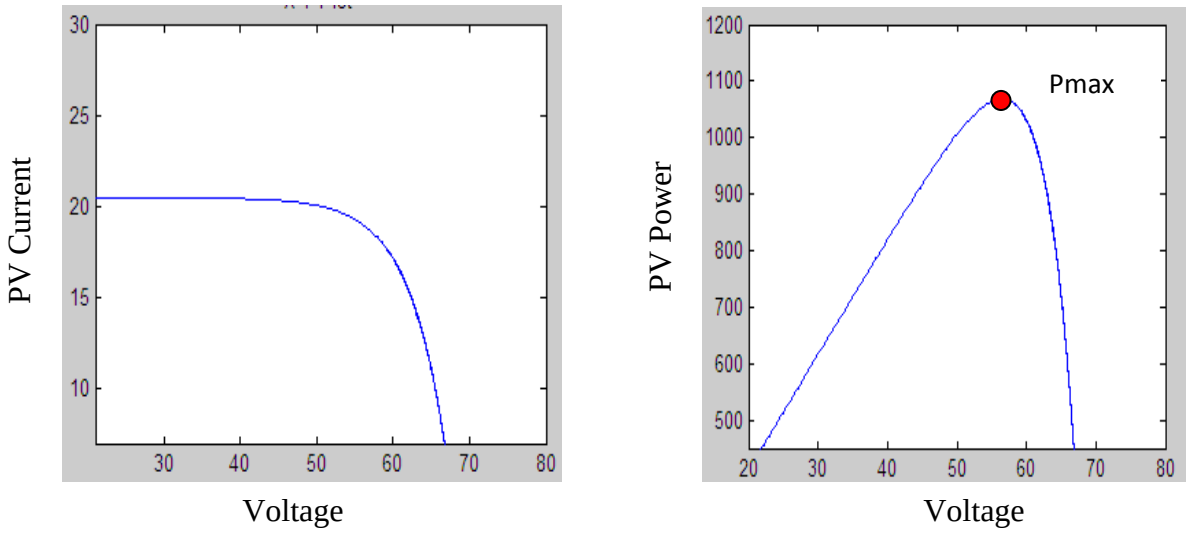


**Fig5.1 (a) Photovoltaic Module I-V curve and(b) P-V curve**

The maximum temperature is 1100 watts i.e Pmax. It occurs around 57volts Vmax, and current is around 21 amps Imax at 400 irradiance as it is clear from figure 5.1(a) & (b).

### 5.3 Simulation Results of Solar Powered Separately Excited DC Motor

This photovoltaic model has to be connected to DC motor via boost converter, then for attaining maximum efficiency; a MPPT (maximum power point tracker) is being employed. Thus the Fig.5.2(a) shows the maximum output power of MPPT i.e 1100watts and the maximum voltage at which it occurs 57 volts as shown in Fig.5.2(b). This input voltage is given as i/p to boost converter.

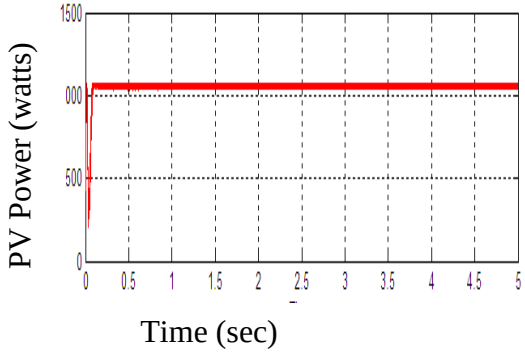


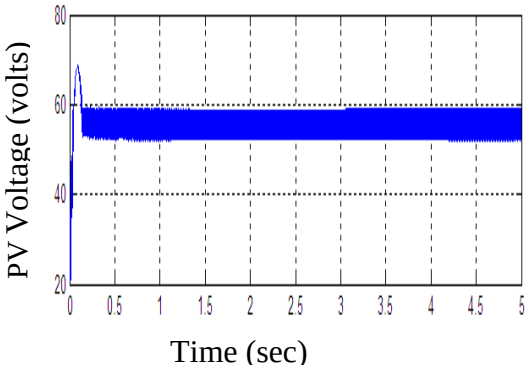


**Fig-5.2(a) The MPPT output power (Pmax)** **(b) and Maximum Voltage (Vmax)**

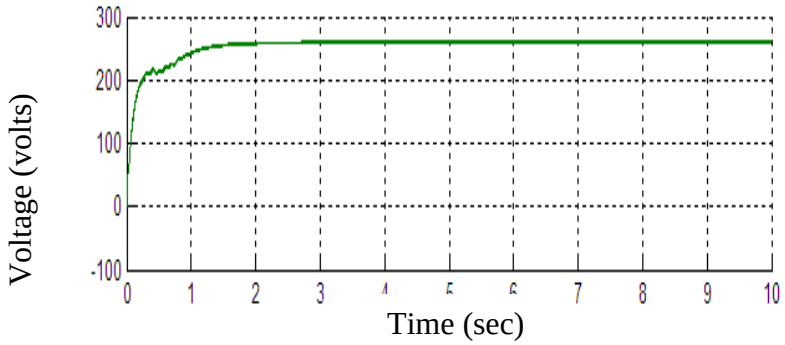


**Fig-5.3 The Boost Converter O/P Voltage**

The figure 5.3 shows the stable output DC voltage of boost converter which is used to as input by the DC motor. The DC motor used is driven for no load conditions and for centrifugal pump load. The output DC voltage is seen nearly around 250 volts.

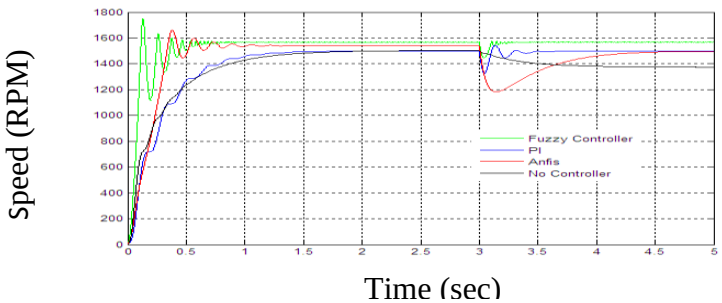


**Fig. 5.4 (a) Output Speed of DC Motor with Different Controllers on NO load (t=0-3 sec) Condition and on Loaded Condition (t=3-5 sec)**

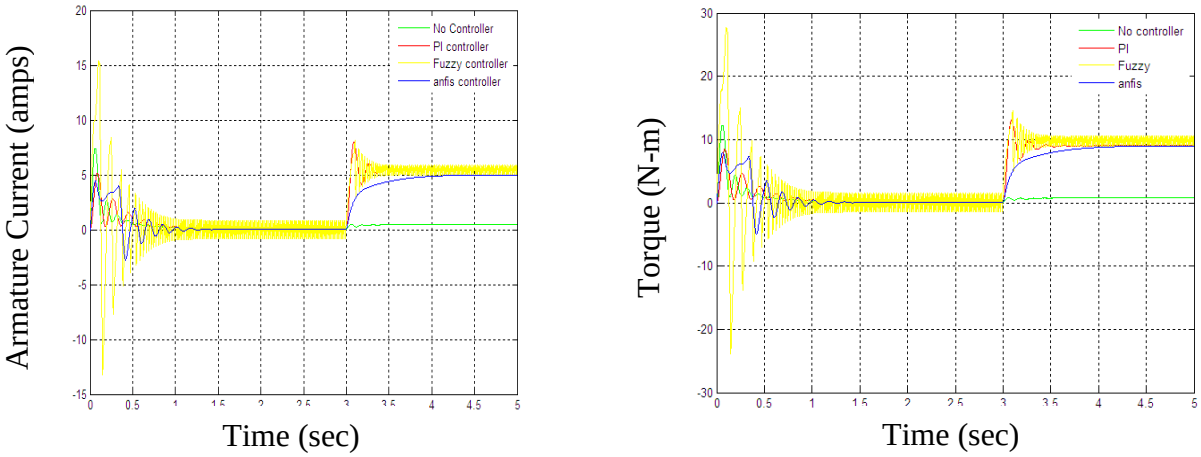


**Fig-5.4(b) Output armature current of DC motor loaded at t=3 sec.**

**(c) Electromagnetic torque of DC motor loaded at t=3 sec.**

Fig 5.4 (a) shows speed of DC motor when the load is applied at t=3 sec the speed of motor decreases at that instant, and the control action is performed by different controllers and the speed again reaches to the rated speed, i.e 1500 rpm. The speed does not reach to 1500 rpm only in case where no controller is applied i.e it remains 1380 rpm. The comparison of different controllers will be discussed later in this chapter.

Fig 5.4(b) and (c) shows variation in armature current and torque developed by the motor, with different controllers. This can be clearly seen that under loaded condition current drawn by the motor increase and thus the torque developed also increases.

**Table 5.1(a) Comparison of Different Controllers under NO Load condition**

| Types Of Controller | Rise Time | Peak Time | Settling Time | Overshoot |
|---|---|---|---|---|
| **PI** | 0.5 sec | - | 2.2sec | - |
| **ANFIS** | 0.28 sec | 0.38 sec | 1.98 sec | 2.6% |
| **FUZZY** | 0.1 sec | 0.12 sec | 1sec | 4.4% |

**Table 5.1(b) Comparison of Different Controllers under Loaded condition**

| Types Of Controller | Peak Time (undershoot) | Settling Time | Undershoot |
|---|---|---|---|
| **PI** | 3.06 sec | .8sec | 6.3% |
| **ANFIS** | 3.15 sec | 2.5 sec | 6.3% |
| **FUZZY** | 3.05 sec | 1sec | 3.3% |

Thus from the above table as shown in table 5.1 (a) under no load condition it become clears that the rise time of PI controller is maximum , having setting time of 2.2sec with no overshoot. Whereas fuzzy controller has smallest rise time with maximum overshoot and settling time of 1sec. So, it becomes clear from the table that compromise has to made on account of rise time or overshoot depending on the application. ANFIS showed results that lie between PI and Fuzzy controller results, thus it best controller for use in speed control of DC motor.

Table 5.1 (b) shows the response of different controllers when the load is applied at t-=3 sec. The PI controller settles fastest, giving large undershoots whereas the fuzzy controller gives the least undershoot. Thus the design of the entire controller depends on application for which it has to be used.

## 5.4 Simulation Results of 0.5 Hp Solar Powered Three Phase Induction Motor Drives

MPPT is used for tracking the maximum power from PV module of given irradiance and temperature. In this simulation, the environmental condition under which the PV module is used is, 400 W/$m^2$ irradiance and $25^0$C, giving the maximum output power of nearly 730 Watts as shown in Fig 5.5. This DC output power generated from PV module is given to 0.5 HP induction motor through inverter circuit.

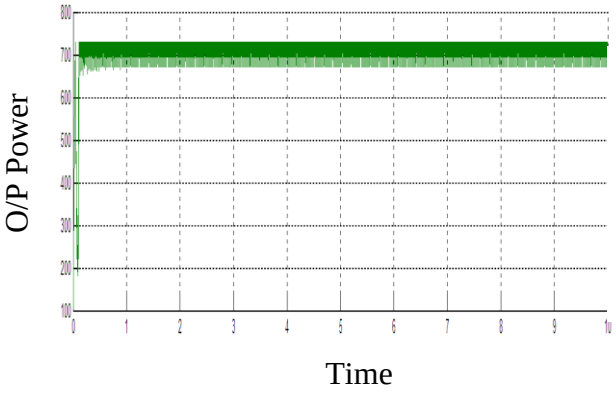


**Fig 5.5 Maximum Power Output of PV module**

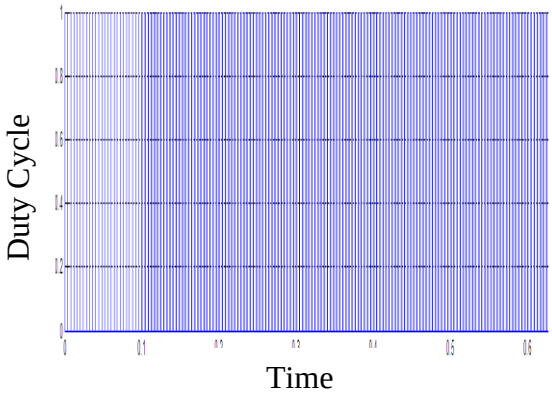


**Fig 5.6 Duty cycle signal generated from MPPT controller**

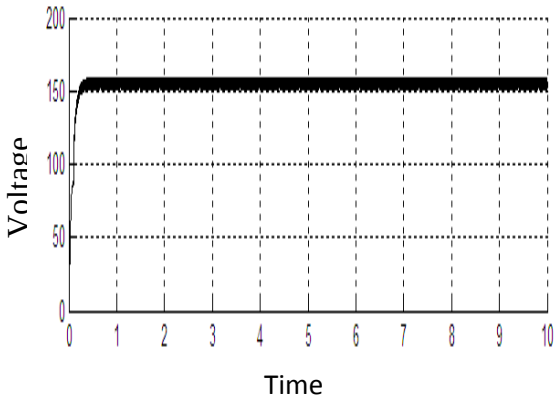


**Fig 5.7 DC Output voltage of Boost Converter**

Once the maximum power is tracked down, duty cycle signal is generated as shown in Fig 5.6. This time varying duty cycle generated is given as switching signal to the gate of MOSFET of boost converter. The switching of MOSFET and the values of inductor

and capacitor selected governs the output voltage and the voltage ripple in the boost converter.

The maximum output voltage produced by PV module is around 78 volts, which is then boosted to 150 volts DC (average value) as shown in fig 5.7 for getting line to line AC voltage of around 110 volts (rms value) .

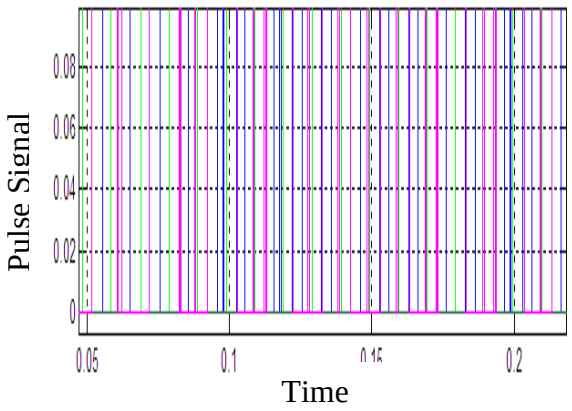


**Fig 5.8 Six pulse PWM fed to gate of inverter**

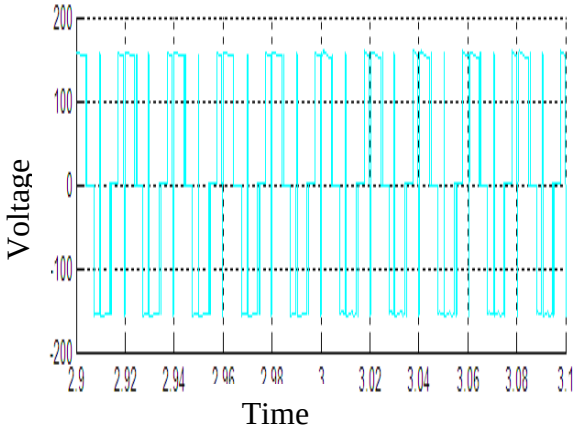


**Fig 5.9 Output voltage of Inverter**

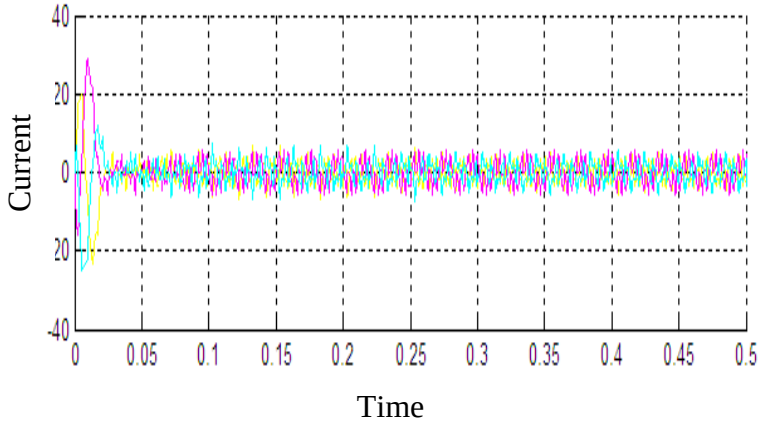


**Fig 5.10 Three phase current wave form of induction motor**

The PWM (pulse width modulation) signal is obtained as shown in fig 5.8 by vector control technique of induction motor. Hysteresis controller is designed to compare the three phase actual current with the three phase reference current developed by vector control technique. Six pulse PWM signal generated is by three phase currents and three by inverting the output. The variation in output voltage of inverter is shown in Fig5.9 which is

given to induction motor. removing the transients is input voltage, as transients badly affect the performance of induction motor.

Initially the current drawn by three phase induction motor is high,( maximum value around 22 amps) for developing the starting torque as shown in figure 5.10. Since the load torque is minimum we see a small current of maximum value 4amps is required for running the 0.5 hp induction motor**.**

### 5.4.1Condition when Load is applied.

On application of centrifugal pump at t=7 sec motor stars drawing more current around 8 amps maximum value as shown in figure 5.26.on further increase in load torque motor starts drawing more current.

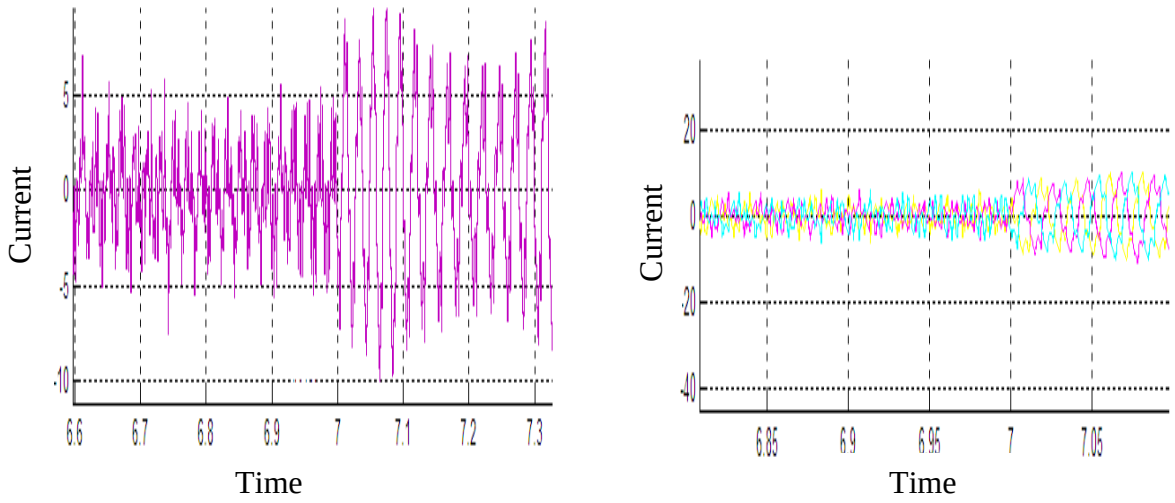


**Fig 5.11(a) Increase in phase current on application of load.**

**5.11(b) Increase in three phase current waveform of motor when load is applied.**

Speed of induction at no load is almost equal to synchronous speed i.e 1500 RPM because the slip at no lad is usually less than 0.5%. But at t=7 sec sec of simulation the machine is loaded with small cenntrifigual pump as a result the rotor speed of induction motor decreases to 1380 RPM as shown in figure 5.12.The slip is now 8%.

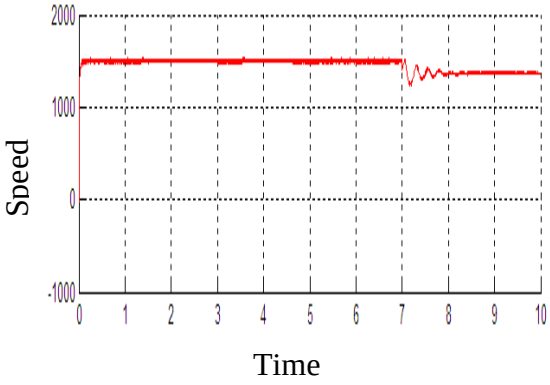


**Fig 5.12 Speed curve of induction motor**

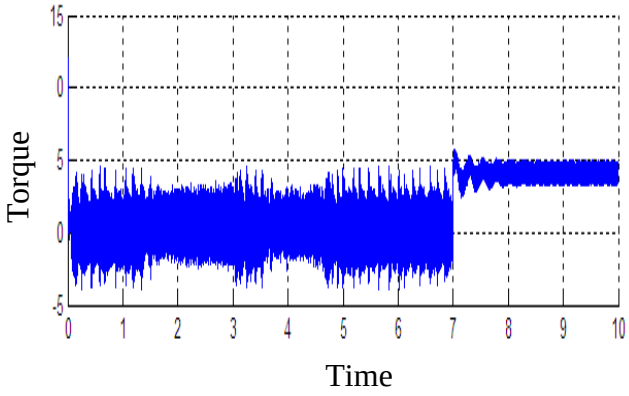


**Fig 5.13 Electromagnetic torque of induction motor**

The electromagnetic torque has minimum value when motor is running at no load i.e torque required to just overcome inertia of motor. But as the machine is loaded with centrifugal pump, the electromagnetic torque developed is 5 N-m as shown in figure 5.13.

### 5.4.2Control Action performed by various Controllers.

Several controllers have been designed for the purpose of speed control of induction motor. Effects of these controllers on speed, and torque of the motor will be clearly seen. On application of load at t=1.5 sec the speed of the motor falls the controller then works to help the motor attain its nominal speed as shown in Fig.5.14(a)

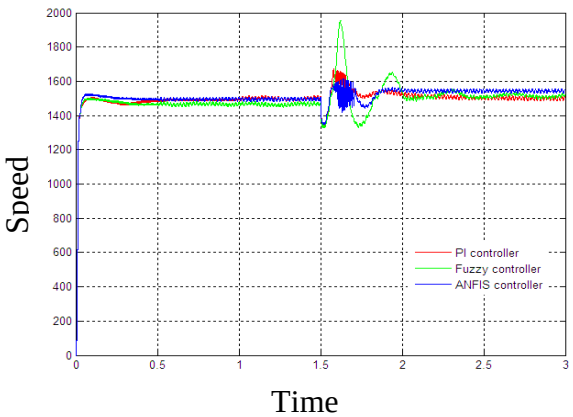


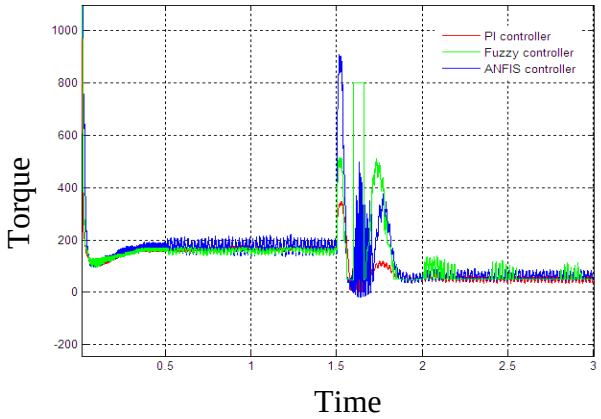


**Fig5.14 (a) Speed with different controllers (b) Torque with different controllers**

The torque developed by the motor when different controllers are taken into account is shown in Fig.5.14(b).

**Table 5.2(a) Comparison of Different Controllers under NO Load condition n**

| Types Of Controller | Rise Time | Peak Time | Settling Time | Overshoot |
|---|---|---|---|---|
| **PI** | 0.016 sec | - | 1 sec | - |
| **ANFIS** | 0.016 sec | - | 0.6 sec | - |
| **FUZZY** | 0.016 sec | 0.07 sec | 0.5 sec | 1.67% |

**Table 5.2(b) Comparison of Different Controllers under Loaded condition**

| Types Of Controller | Peak Time (undershoot) | Settling Time | Undershoot |
|---|---|---|---|
| **PI** | 1.52 sec | 1sec | 5% |
| **ANFIS** | 1.52 sec | 1.5 sec | 3.5% |
| **FUZZY** | 1.52 sec | 2.6%(offset) | 6% |

Thus, the performance of PI controller was exceptionally good in both the above cases as shown in table 5.2 (a) & (b). But Fuzzy and ANFIS Controller do performed satisfactorily, and can be designed more precisely based on the expert knowledge.. Thus, all the above controllers can be used for speed control of induction motor depending on application and knowledge of the system available.

# CHAPTER IV

# CONCLUSION AND FUTURE SCOPE OF WORK

Thus from the above results as shown in Chapter V it becomes clear that design of solar powered electric drive is an efficient work, and is helpful for pumping application even in remote areas. All the design parameters, procedures and results have been discussed in detail in previous chapters. Different controllers used are compared on the basis of their computational efforts and performance.

The scope for future work in this area are discussed below-

(1) Implementation of other MPPT techniques for control of Duty cycle.
(2) Design of other controllers like neural network.
(3) Implementation of other control techniques.

# REFERENCES

[1] Samer Said, Ahmed Massoud, Mohieddine Benammar and Shehab Ahmed, "A Matlab/Simulink-Based Photovoltaic Array Model Employing Sim Power Systems Toolbox", Journal of Energy and Power Engineering,Vol 6, pp 102-106, 2012.

[2] N. Pandiarajan and Ranganath Muthu , "Mathematical modeling of photovoltaic Module with Simulink" International Conference on Electrical Energy Systems, Vol.2, pp 3-7, Jan 2011.

[3] M. Abdulkadir, A.S. Samosir and A.H.M. Yatim, "Modeling and Simulation Based Approach of Photovoltaic System in Simulink Model", ARPN Journal of Engineering and Applied Sciences, Vol. 7, No.5,pp 616-623, May 2012.

[4] Kinal Kachhiya and MakarandLokhande, "Matlab/ Simulink Model of Solar PV Module and MPPT Algorithm", National Conference on Recent Trends in Engineering and Technology, Vol.2, pp. 1-5, 13-14 May 2011.

[5] Tarak Salmi, Mounir Bouzguenda, Adel Gastli and Ahmed Masmoudi, "Matlab/ Simulink Based Modelling of Solar Photovoltaic Cell", International Journal of Renewable Energy Research, Vol. 2, No. 2, pp 213-217, 2012.

[6] PatilSahebrao N. and R.C. Prasad, "Design and Simulation of MPPT Algorithm for Solar Energy System using Simulink Model", International Journal of Research in Engineering and Applied Sciences(IJREAS), Vol. 02, No.1,pp 37-40 , January 2014.

[7] Biji.G., "Modelling and Simulation of PV Based Pumping System for Maximum Efficiency", IEEE conference on Application of Industrial Systems, Vol. 9, pp 449- 454 August 2012.

[8] Johan H.R. Enslin, Mario S. Wolf, Daniel B. Snyman and WernherSwiegers, "Integrated Photovoltaic Maximum Power Point Tracking Converter", IEEE Transactions on Industrial Electronics, Vol. 44, No. 6,pp 769-773, December 1997.

[9] M. Abdulkadir, A.S. Samosir, A.H.M. Yatim and S.T. Yusuf, "A New Approach of Modelling, Simulation of MPPT for Photovoltaic System in Simulink Model", ARPN Journal of Engineering and Applied Sciences, Vol. 8, No. 7,pp 488-494, July 2013.

[10] E. Skoplaki and J.A. Palyvos, "On the Temperature dependence of Photovoltaic Module Electrical Performance: A review of efficiency/power correlations", Solar Energy, pp. 614-624, 2009.

[11] C. Liu, B. Wu and R. Cheung, "Advanced Algorithm for MPPT Control of Photovoltaic Systems", Canadian Solar Buildings Conference, Montreal, Vol.8, pp-20-24, August 2004.

[12] T.J. McMahon and B. von Roedern, "Effect of Light Intensity on Current Collection in Thin- Film Solar Cells", 26th IEEE Photovoltaic Specialists Conference, Anaheim, California, Vol.6, pp 5-9,September 29- October 3 1997.

[13] Guanghui Li, Xinchun Shi, Chao Fu and Guoliang Zhou, "Design and Implementation of a Novel MPPT Controller Based on Sun Tracking Technology", IEEE, Vol. 3, No. 3, pp. 2611-2615, August 1983.

[14] Karl H. Edelmoser and Felix A. Himmelstoss, " DC-to-DC Solar Converter with Controlled Active Clamping System", IEEE Transaction on power Electronics, Vol.3, pp 124-127, 2006.

[15] Mohan Kashyap, SaurabhChanana and Jai Singh Arya, " Solar Powered PMDC Motor Drive", Conference on Advances in Communication and Control Systems, Vol.3, pp18-22, 2013 .

[16] Ziyad M. Salameh and FouadDagher, "The Effect of Electrical Array Reconfiguration on the Performance of a PV-Powered Volumetric Water Pump", IEEE Transactions on Energy Conversion, Vol. 5, No. 4,pp 653-658, December 1990.

[17] J.Appelbaum , "Starting and Steady state characteristics of DC Motor Powered by Solar Cell Generators", IEEE Trans on Energy Conversion ,Vol 1, No1, pp-17-25,1986.

[18] S.M. Alghuwainem, "Steady-State Performance of DC Motors Supplied from Photovoltaic Generators with Step-Up Converter", IEEE Transactions on Energy Conversion, Vol. 7, No. 2, pp-267-272, June 1992.

[20] Mohamed M. Saied, "A Study on the Matching of DC Motors to Photovoltaic Solar Arrays", IEEE Transactions on Energy Conversion, Vol. EC-3, No. 3, pp.652-655, September 1988.

[21] S. Singer and J. Appelbaum, "Starting Characteristics of Direct Current Motors Powered by Solar Cells", IEEE Transactions on Energy Conversion, Vol. 8, No.1, pp 47-53, March 1993.

[22] S.M. Alghuwainem, "Speed Control of a PV Powered DC Motor Driving a Self-Excited 3-Phase Induction Generator for Maximum Utilization Efficiency", IEEE Transactions on Energy Conversion, Vol. 11, No. 4,pp 768-773 December 1996.

[23] M. Rama Prasad Reddy, T. Bramhananda Reddy and B. Brahmaiah, "Vector Based Hysteresis Current Control Scheme for Vector Controlled Induction Motor Drives", EPE Journal, No.1, pp. 13-18, July 1991.

[24] Adel Aktaibi and DawGhanim, "Dynamic Simulation of a Three-Phase Induction Motor Using Matlab Simulink", IEEE Proceedings, Vol. 129, No. 6, pp. 260-265, November 1982.

[26] N. Ravi Shankar Reddy, T. Brahmananda Reddy, J. Amarnath and D. SubbaRayudu, "Space Vector Based Minimum Switching Loss PWM Algorithms for Vector Controlled Induction Motor Drives", ICGST-ACSE Journal, Vol. 10, No. 1, pp. 39-48, November 2010.

[27] Gilberto C.D. Sousa, Domingos S.L. Simonetti, Ever E.C. Norena, "Efficiency Optimisation of a Solar Boat Induction Motor Drive", IEEE Transactions on Industrial Electronics, Vol. 42, No. 2, pp. 1424-1430, April 1995.

[28] Aurobindo Panda, M.K. Pathak and S.P. Srivastava, "Solar Direct Torque Controlled Induction Motor Drive for Industrial Applications", International Journal of Renewable Energy Research, Vol. 3, No. 4, pp 794-802,2013.

[29] M. Arrouf and N. Bouguechal, "Vector Control of an Induction Motor fed by a Photovoltaic Generator",Applied Energy 74, pp.159-167, 2003.

[30] J.A. Santiago- Gonzalez, J. Cruz- Colon, R. Otero-De-Leon, V. Lopez-Santiago and E.I. Ortiz-Rivera, "Three Phase Induction Motor Drive Using Flyback Converter and PWM Inverter Fed from a Single Photovoltaic Panel", M.S. Dissertation, University of Puerto Rico, Mayaguez Campus, Vol.6,pp 1-6, December 2009.

[31] OlorunfemiOjo, "Analysis of Current Source Induction Motor Drive fed from Photovoltaic Energy Source", IEEE Transactions on Energy Conversion, Vol. 6, No.1, pp 99-106, March 1991.

[32] B.N. Singh, Bhim Singh, B.P. Singh, A. Chandra and K.Al-Haddad, "Optimised Performance of Solar Powered Variable Speed Induction Motor Drive", Conference Proceeding, 16th International Conference on Power Conversion and Intelligent Motion (PCIM'94), Nurnberg, Germany, Vol. 8,pp 58-66, June 28th to 30th 1994.

[33] A.Abbou, T. Nasser, H. Mahmoudi, M. Akherraz and A. Essadki, "Induction Motor Controls and Implementation using dSPACE", WSEAS Transactions on Systems and Control, Vol. 3, No. 1, pp. 166-173, January- February 2008.

[34] N.K. Lujara, J.D. van Wyk and P.N. Materu, "Loss Models of Photovoltaic Water Pumping Systems", IEEE International Symposium in Industrial Electronics, Pretoria, pp 965-970, 7-10 July 1998.

[35] I.H. Atlas and A.M. Sharaf, "A Novel GUI Modeled Fuzzy Logic Controller for a Solar Powered Energy Utilization Scheme", Electric Power Systems Research Journal, Vol. 25, No. 3, pp. 227-232, 1992.

[36] R.C. Zowarka, T.J. Hotz, J.R. Uglum and H.E. Jordan, "Induction Motor Performance Testing with an Inverter Power Supply, Part 2", IEEE Transactions on Magnetics, Vol. 43, No.1, pp. 275-278, January 2007.

[37] P. Ragot, M. Markovic and Y. Perriard, "Optimization of Electric Motor for a Solar Airplane Application", IEEE-IEMDC Conference, Sant-Antonio(USA), Vol. 9, pp 1487-1493,May 2005.

[38] Hiroaki Yamamoto, Kohji Tanaka and Ichiro Miki, "An Auto-Tuning Method for Vector Controlled Induction Motor Drives Considering Stator Core Loss", Transactions IEEE Japan- Industrial Application Society, Vol. 109-D, No. 11, pp. 97-102, 2005.

[39] K. Naga Sujatha and K. Vaisakh, "Implementation of adaptive neuro fuzzy inference system in speed control of induction motor" IEEE Tansaction on Industrial Application, Vol.2, pp. 110-118, 2010.

[40] B. Venkata Ranganadh, A. Mallikarjuna Prasad and Madichetty Sreedhar, "Modelling and Simulation of a Hysteresis Band Pulse Width Modulated Current Controller Applied to a Three Phase Voltage Source Inverter by using Matlab", International Journal of Advanced Research in Electrical, Electronics and Instrumentation Engineering, Vol. 2, No.9, pp 4378-4387,September 2013.

[41] Nelson Mendez-Gomez, Orlando Bousono, Ricardo Castaneyra and Eduardo I. Ortiz-Rivera, "Development of a Low Cost Induction Motor Drive System using a PVM, Boost Converter and Three-Phase Inverter", IEEE Conference on Industrial Application Society, Vol.4, 2011.

[42] Vongmanee V., Monyakul V. and Youngyuan U., "Vector Control of Induction Motor Drive System supplied by Photovoltaic Arrays", IEEE Transaction on Energy conservation, Vol.8, 2002.

[43] A.M. Sharaf, E. Ozkop and I.H. Atlas, "A Hybrid Photovoltaic PV Array-Battery Powered EV-PMDC Drive Scheme", IEEE International Symposium on Industrial Electronics, ISIE'95,Vol.72, pp.272-278, 1995.

[44] Joshua Anzicek and Mark Thompson, "DC-DC Boost Converter Design for Kettering University S Gem Fuel Cell Vehicle", Proceedings of the 3rd International Conference on Fuel Cell Science, Engineering and Technology, Ypsilanti, pp 307-316, May 2005.

[45] Ulrich Herrmann, Hans Georg Langer and Heinz van der Broeck, "Low Cost DC to AC Converter for Photovoltaic Power Conversion in Residential Applications", IEEE Transactions on Industrial Applications, Vol. IA-19, No. 2, pp 588-594, March/April 1983.

[46] B.A.A. Omar , A.Y.M. Haikal, F.F.G. Areed, "Design adaptive neuro-fuzzy speed controller for an electro-mechanical system" Ain Shams Engineering Journal ,2011, vol.2, pp-99–107.

[47] Rekha kushwah, Sulochana Wadhwani, "Speed Control of Separately Excited Dc Motor Using Fuzzy Logic Controller," International Journal of Engineering Trends and Technology, Vol.4, No. 6,pp 2518-2523, June 2013.

[48] R. P. Suradkar, Dr. A. G. Thosar," Enhancing the Performance of DC Motor Speed Control Using Fuzzy Logic," International Journal of Engineering Research & Technology , Vol. 1, No. 8, pp 119-124, October 2012.

[49] Rasoul Rahmani, M.S. Mahmodian, Saad Mekhilef, Member,and A. A. Shojaei, "Fuzzy Logic Controller Optimized by Particle Swam Optimization for DC Motor Speed Control," IEEE student conference on Rescerch and Development, Vol.6, pp 23-28, 2012.

[50] Philip A. Adewuyi, "DC Motor Speed Control: A Case between PID Controller and Fuzzy Logic Controller," International Journal of multidisciplinary sciences and engineering, Vol.4, No.4, pp 657-662, May 2003.

[51] Salim, Jyoti Ohri, Naveen, " Speed Control of DC Motor using Fuzzy Logic based on LabVIEW," International Journal of Scientific and Research Publications, Vol.3, No.6,pp 234-240, June 2013.

[52] Atul Kumar Dewangan,, Sashai Shukla, Vinod Yadu, "Speed Control of a Separately Excited DC Motor Using Fuzzy Logic Control Based on Matlab Simulation Program," International Journal of Scientific & Technology Research Vol. 1, No. 2,pp 13-19, March 2012.

# APPENDIX

**Table1- Parameter specification of PV module**

| | | |
|---|---|---|
| Maximum power | Pm | 1260 |
| Maximum voltage | Vm | 54.2 |
| Current at max power | Im | 23.25 |
| Open circuit voltage | Voc | 66 |
| Short circuit current | Isc | 25.44 |
| Total series resistance | Rsh | 2.2Ω |

**Table 2 Parameter specification of DC Motor**

| | |
|---|---|
| **Motor Type** | Separately Excited |
| **Rated Armature Voltage** | **260V** |
| **Rated Armature current** | **3.3A** |
| **Rated Speed** | **ω=157 rad/sec.** |
| **Armature Resistance** | **1.9Ω** |
| **Armature Inductance** | **0.18H** |
| **Mutual Inductance** | **1.2H** |
| **Motor rotational Loss** | **TL=0.2+0.0015 ω N-m** |
| **Pump type** | **Centrifugal** |
| **Rated torque** | **TP= 0.001 ω^1.8 N-m** |
| **Pump rotational Loss** | **TL=0.3+.0025 ω** |

**Cage Motor Specifications: 0**.37kW (0.5hp), Y-connected, 110v, 3.5A, Ra=1.18Ωs, Rs=1.47Ωs, $X_{ls}$=1.38Ωs, $X_{lr}$=1.38Ωs, M=0.135H, $X_m$=43.65Ωs and J=0.0018 Kg-$m^2$.